Received: 16 April 2018 | Revised: 18 June 2018 | Accepted: 27 June 2018

DOI: 10.1111/geb.12805

RESEARCH PAPER

WILEY Global Ecology and Biogeography A Journal of Macroecology

Thermal constraints on body size depend on the population's position within the species' thermal range in temperate songbirds

Nicolas Dubos[1,2] | Olivier Dehorter[1] | Pierre-Yves Henry[1,2*] | Isabelle Le Viol[1,3*]

[1]Centre d'Ecologie et des Sciences de la Conservation (CESCO UMR 7204), Centre de Recherches sur la Biologie des Populations d'Oiseaux (CRBPO), Sorbonne Universités, MNHN, CNRS, Paris, France

[2]Mécanismes adaptatifs et évolution (MECADEV UMR 7179), Sorbonne Universités, MNHN, CNRS, Brunoy, France

[3]Centre d'Ecologie et des Sciences de la Conservation (CESCO, UMR 7204, CNRS, MNHN, Sorbonne-Université, MNHN, Station marine de Concarneau, France

Correspondence

Nicolas Dubos, CESCO UMR 7204, Muséum national d'Histoire naturelle, 43 rue Buffon, CP 135, 75005 Paris, France.
Email: dubos.research@gmail.com

Funding information

LabEx BCDiv; Ministry of Environment; FP6

Editor: Shai Meiri

Abstract

Aim: There is mounting evidence that climate warming can induce morphological changes locally, particularly size reduction. However, the direction of thermal stress may differ between climatic regions. We predicted that morphological response to temperature fluctuations should vary throughout species ranges, depending on the local climate. Hot temperature anomalies are expected to induce size reduction in hot regions where species live close to their upper thermal limit, whereas size stasis (or increase) would be expected in cold regions, where species live close to their lower thermal limit.

Location: France (204 sites).

Time period: 2000–2014 springs.

Major taxa studied: Songbird species (n = 9).

Methods: We tested whether the effect of temperature anomalies on juvenile body size varied along an 11 °C thermal gradient.

Results: In warmer springs, juveniles were larger overall at the coldest sites, but this effect decreased toward the hottest sites, becoming negative for two species.

Main conclusions: Warming should induce body size increases more frequently at the cold edge of species distribution ranges, and rather body size declines at the hot edg. The climate dependency of the effect of weather fluctuations on body size is still under-acknowledged, and the pattern identified deserves to be investigated over broader climatic gradients and taxonomic coverage. Climate-driven changes in body size are therefore not uniform across climatic regions and within species ranges.

KEYWORDS

Bergmann's rule, birds, climate warming, France, temperature anomaly, thermal range, wing length

1 | INTRODUCTION

Although increasing attention is now being given to body size change as a response to climate warming (Gardner, Peters, Kearney, Joseph, & Heinsohn, 2011), this phenomenon is still little documented and its underlying mechanisms are poorly understood. The effects of rising temperatures on animal structural size can be mediated through effects on juvenile growth and size-dependent mortality. The original proposal was that body size would decline with warming as a result of the advantage of being smaller under warmer conditions. With a

---

*These authors contributed equally.

higher surface–volume ratio, smaller individuals can dissipate body heat more efficiently than larger individuals, which is advantageous in warm climates, as stated in Bergmann's rule (Bergmann, 1847). With climate warming, larger individuals would increasingly suffer from hyperthermia, and a size reduction is a possible adaptive response enabling individuals to cope with increasingly warm conditions (Gardner et al., 2011).

The application of Bergmann's rule to climate warming has received controversial evidence so far (Teplitsky & Millien, 2014). Despite rising temperatures, many species have not exhibited any change in body size over time (Kruuk, Osmond, & Cockburn, 2015; Meiri, Guy, Dayan, & Simberloff, 2009), whereas in others, the recorded trend is opposite to the prediction, that is, a size increase has occurred (Björklund, Borras, Cabrera, & Senar, 2014; Pérez et al., 2016). This may be related to the complexity of temperature and other climatic impacts on physiology and body size (Gardner, Amano, Mackey, et al., 2014). Temperature change can potentially have contradictory effects depending on which biological feature is affected (e.g., body growth versus survival), and which aspect of temperature change is regarded (e.g., mean temperature versus heat wave frequency). For instance, increasing mean temperatures may impact body growth positively, which is contradictory to the proposal of an application of Bergmann's rule to climate warming (i.e., selection for smaller in warmer mean temperatures). Besides, heat waves may select for larger individuals as a result of a lower evaporative water loss, enabling them to better evade dehydration (Gardner et al., 2011). More importantly, the effect of temperature fluctuations probably differs between climatic regions. For instance, the physiological and ecological consequences of annual weather deviation are likely to depend on the average local climatic regime: in cool or cold regions (e.g., Collins, Relyea, Blustein, & Badami, 2017a; Dubos et al., 2018; Pérez et al., 2016), or during cool periods of the year (e.g., Gardner, Amano, Mackey, et al., 2014), hot temperatures indeed affect body growth positively. In addition, events of extreme heat are also scarcer in temperate climates than in arid systems (Garcia, Cabeza, Rahbek, & Araújo, 2014). Observed body size variations are therefore expected to represent the response to fluctuations in average temperatures in temperate climates (Dubos et al., 2018), whereas the influence of extreme hot events is expected to be particularly strong in arid, semi-arid and tropical climates (Gardner et al., 2017; Holmgren et al., 2016). In arid or semi-arid climates, larger individuals are expected to survive heat waves better, presumably because the smallest individuals show higher rates of evaporative water loss, and would be more exposed to dehydration and mortality during heat waves (McKechnie & Wolf, 2010).

For the same species, temporal variation in body size can differ between sites (e.g., Collins et al., 2017a; Dubos et al., 2018; Meiri et al., 2009). Within a species' distribution range, populations are likely to have adapted locally to average meteorological conditions (e.g., Both & te Marvelde, 2007). Their response to changes in environmental conditions may therefore differ between the hottest and the coldest parts of their distribution range (Both & te Marvelde, 2007; Socolar, Epanchin, Beissinger, & Tingley, 2017). This is the case for population trends of European birds: abundances decline toward the hot edge of their species' distribution range, while they increase toward the cold edge (Jiguet et al., 2010). Differential responses to climate change have also been observed in avian phenology, with advancements in egg laying near the cold edge but not near the warm one (depending on the species; Both & te Marvelde, 2007). A similar pattern was found in the nesting success of Californian birds, with a positive effect of temperature anomaly toward the cold edge of species distributions, and a negative effect toward the warm edge (Socolar et al., 2017). Individuals living close to the hot edge of their species' distribution range are the most threatened by climate warming, because they live close to their upper thermal limit already (Deutsch et al., 2008; Jiguet et al., 2010; Socolar et al., 2017; Tewksbury, Huey, & Deutsch, 2008). Conversely, individuals living at the cold edge are more cold-limited and would even benefit from hot anomalies, as a result of a lower exposure to cold stress (Jiguet et al., 2006). Hence, across thermal ranges, the impact of climate warming on populations is expected to change gradually, and ranges from positive at the cold edge toward negative at the hot edge (Jiguet et al., 2010). The influence of thermal anomalies would therefore depend on the relative position of the population within the distribution range, even within the inner part of species' thermal ranges. Although this variation in the effect of temperature anomalies across a species' range is now well acknowledged for population trends (Jiguet et al., 2010), to our knowledge, it has not yet been investigated for body size responses to temperature changes.

Contrasting effects of temperature increase on body size across the thermal range are expected to occur through two main mechanisms: (a) direct, thermoregulatory costs, and (b) indirect, ecological effects through ecosystem productivity (Yom-Tov & Geffen, 2011) and temporally mismatched predator–prey interactions (Husby, Hille, & Visser, 2011). Firstly, the ability to thermoregulate depends on morphology, and the thermal constraint affecting morphology is expected to depend on the local climate. For instance, in song sparrows (*Melospiza melodia*), selection for heat retention was found to prevail in a continental climate during winter (Danner & Greenberg, 2015), while for the same species, it was driven by heat dissipation in a Mediterranean climate during summer (Greenberg, Cadena, Danner, & Tattersall, 2012). In this case, the differential morphological change affecting thermoregulation was applied to bill size. However, this should also apply to structural size, as heat loss/conservation can depend on the size of body appendices (e.g., Allen's rule; Allen, 1877) as well as on structural size (e.g., Bergmann's rule). In cold or cool regions (e.g., temperate to polar), individuals may be larger in warmer years (Collins et al., 2017b; Dubos et al., 2018; Pérez et al., 2016) when the cold constraint on growth is alleviated. Tissue growth increases with temperature in two ways: by accelerating biochemical reactions and metabolism (Gillooly, Brown, West, Savage, & Charnov, 2001), and by reducing the allocation of energy used for body heat maintenance (Kendeigh, 1969), so this energy can be reallocated to growth (Dawson, Lawrie, & Brien, 2005; Gillooly et al., 2001). Nestling growth may also be indirectly facilitated by warmer temperatures through the reduced thermoregulatory load

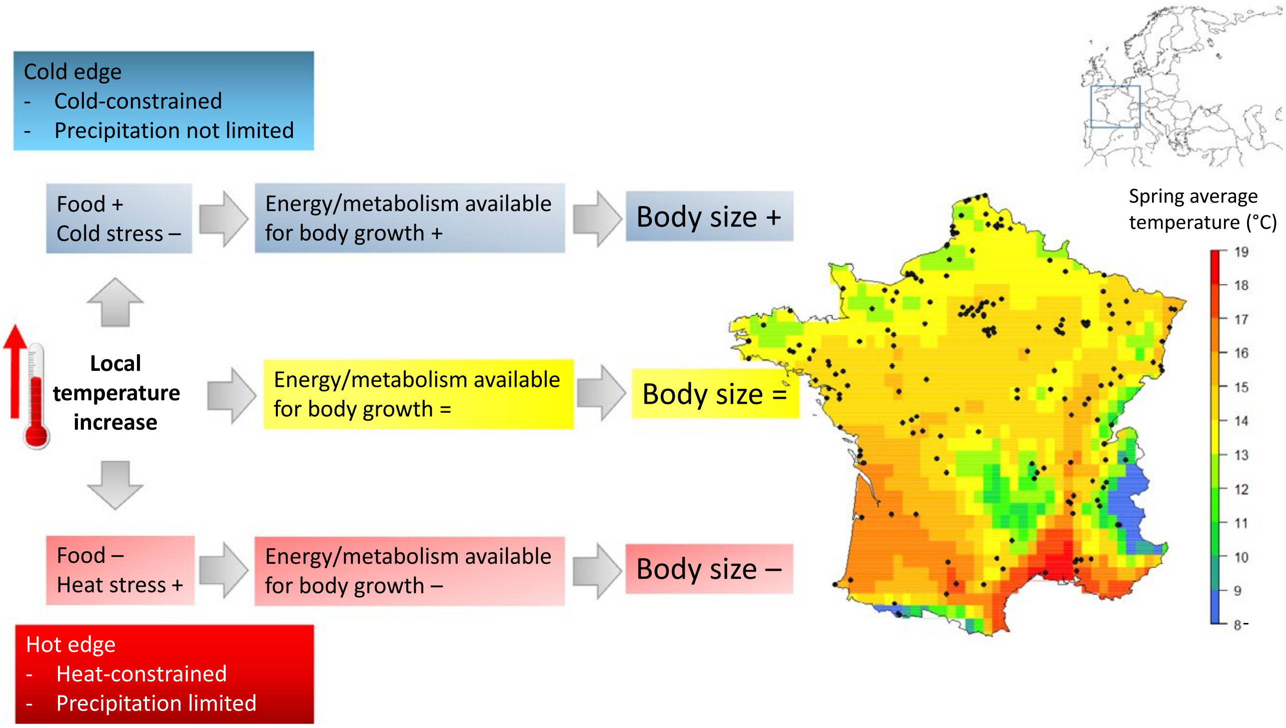

FIGURE 1 Theoretical framework for a differential effect of climate warming on body size depending on local climate (here, spring average temperatures). At hot sites (red, dark orange, including the Mediterranean region), positive temperature anomalies are predicted to induce body size reduction, whereas at cool sites (blue-green, including mountain regions), body size enlargement is expected. The map shows the distribution of the 204 study sites in France [Colour figure can be viewed at wileyonlinelibrary.com]

for parents: parents can spend more time foraging to provision nestlings with food, and less time at the nest to keep them warm (e.g., Socolar et al., 2017). In warmer regions (e.g., dry tropical and Mediterranean), the risk that a temperature increase reaches detrimental or sub-lethal levels is higher (Khaliq, Hof, Prinzinger, Böhning-Gaese, & Pfenninger, 2014). Larger individuals may suffer more from increasing temperature, as interpreted with the application of Bergmann's rule to warming (Gardner et al., 2011). Secondly, body size depends on food availability during ontogeny. For secondary consumers, food availability depends on temperature-driven primary production (Yom-Tov & Geffen, 2011). In temperate regions, precipitation is rarely limiting, and higher temperatures would increase invertebrate abundance, that is, the main resource for nestling and fledgling songbirds (Bale et al., 2002; but see Carroll et al. 2015 for an opposite response in hygrophilic peatlands). In semi-arid systems, such as Mediterranean regions, invertebrate abundance is more constrained by drought, resulting from limited rainfall combined with high temperatures. An increase in spring temperature may therefore result in larger body size in cool climates, whereas it could result in smaller body size in Mediterranean or dry tropical climates, in the case of co-occurrence with limited precipitation. Hence, direct and indirect effects of temporal variation in mean temperature on body size are expected to differ between the hottest and the coldest parts of species ranges (Figure 1).

We assessed whether the effect of interannual variation in mean spring temperature on juvenile body size varies along a thermal gradient (11.2 °C between the coldest and the hottest study sites; Figure 1) in a temperate region (France) for nine songbird species. We predicted that, during hot springs (relative to the local average temperature), juveniles should be larger at the coldest sites, and smaller at the hottest sites (Figure 1). In temperate climates, the tipping-point of the effect of local temperature on body size sensitivity to temperature anomalies should depend on the position of populations within the species' thermal ranges: the colder the location of a population, the more its growth should increase with temperature anomaly.

2 | METHODS

2.1 | Bird survey

We used individual records of songbirds caught during sessions of the French Constant bird ringing Effort Sites (CES) scheme, from 2000 to 2014 (Robinson et al., 2009; more information at https://crbpo.mnhn.fr, see 'STOC Capture'). Biometric data used in the present study were collected at 204 sites by 132 volunteer bird ringers, each site being monitored during 4.1 ± 3.3 *SD* years (Dehorter & CRBPO, 2017). Each site was visited at least three times during the breeding season (average 3.6 ± 1.6 *SD*), from 15 May until 19 July. For a given site, number and location of mist-nets were kept constant throughout the years. Each captured individual was individually marked, identified to species and aged (juvenile for birds born during the ongoing breeding season; Svensson, 1992). Most sites are located in shrublands, woodlands with dense understorey, or reedbeds (Eglington et al., 2015). Our survey encompassed three major types of climate based on the Köppen Geiger classification (Peel, Finlayson, & McMahon, 2007): subalpine (corresponding to the subarctic climate, Dfc), temperate oceanic (Cfb), and hot-summer Mediterranean climates (Csa), with a thermal range of 11.2 °C between the coldest (8.4 °C on average) and the hottest sites (19.6 °C on average; Figure S1) during spring.

2.2 | Biometric data

Wing length measurements were used as a proxy for body size (Gosler, 1998; data for supposedly better proxies of body size, such as tarsus or longest feather lengths were not available, and body mass data convey information on precipitation-dependency of body condition rather than on temperature-dependency of body size, see Dubos et al., 2018). We worked on post-fledgling juveniles only, because individual body size is determined during a short period of growth in small songbirds, taking place mainly during the nestling stage (*c*. 2–3 weeks), and continuing for a few weeks after fledging (Salewski, Hochachka, & Fiedler, 2010; Yom-Tov & Geffen, 2011). When recaptures occurred (representing 10% of the data), we randomly selected one measurement per individual. In May–July, when captures took place, juvenile songbirds are still within a few kilometres from their birth site, and captured individuals can be assumed to have grown under the documented local climatic conditions. Adults were not considered as their wing length depends on multiple, confounding effects of climate throughout the life cycle (ontogeny, yearly moult and size-dependent mortality; Yom-Tov & Geffen, 2011).

As small sample sizes and data sparseness can compromise the robustness of inferences (Yom-Tov & Geffen, 2011), we decided to include data for only (a) species with ≥ 1,000 measured individuals, and (b) species.site.year sampling units with ≥ 10 measured individuals (Table S1). As the hypotheses to be tested required that the position of each population within the relevant species' thermal range varied across sampling sites (i.e., gradient of 'northern'/core/'southern' populations), we measured the proportion of each species' thermal range that was included in our study area. To do this, we relied on the population's thermal coordinate (Jiguet et al., 2010), an index of the relative position of a given site, for a given species, within its European thermal range (Table S1; Figure S1). A population's thermal coordinate is computed as the difference between the species' thermal maximum (mean spring temperature of the hottest 5% of European Atlas grid cells; Jiguet et al., 2010) and the average temperature of a given site, divided by the species' thermal range (°C). This index varies between 0 and 1. Values close to 0 represent populations near the species' thermal minimum; values closer to 1 are populations near the species' thermal maximum. We discarded one species (*Acrocephalus schoenobaenus*) because the thermal gradient represented by the study sites was very narrow (2.2 °C between the coldest and the hottest sites, representing less than 15% of the species' thermal range). For the remaining species, a wider proportion of their thermal range was represented (minimum for *Sylvia communis* = 31%, representing a thermal gradient of 4.2°; respectively, mean = 58% ± 13 *SD* and 8.5°C ± 2.3 *SD* for all species in Table S1). For seven species, surveyed sites fell well within the species' thermal range (and edges were not documented), whereas for two species (long-tailed tit, *Aegithalos caudatus*; common chiffchaff, *Phylloscopus collybita*), some sites corresponded the hot edge of their respective thermal ranges. According to habitat preference, one species is a reedbed specialist (common reed-warbler, *Acrocephalus scirpaceus*), whereas the eight others are shrubland/woodland generalists (great tit, *Parus major*; Eurasian blue tit, *Cyanistes caeruleus*; Eurasian blackcap, *Sylvia atricapilla*; common whitethroat, *Sylvia communis*; common chiffchaff; long-tailed tit; Eurasian blackbird, *Turdus merula*; and European robin, *Erithacus rubecula*; cf. Table S1, Figure S2). The final dataset included nine species, all living in relatively similar thermal niches, resulting in a total of 34,101 juveniles measured (see details per species in Table S1).

2.3 | Climatic data

We used daily mean temperature data, obtained from E-Obs (Haylock, et al., 2008), and for each site we computed: (a) yearly 'spring temperatures' (denoted as $T_{S.Y}$), that is, the mean temperature of a given year, at the site, for spring (from 1 April to 31 July, documenting between-year fluctuations of local thermal conditions), and (b) 'local average temperature' (denoted as T_s), as the mean of $T_{S.Y}$ over the 2000–2014 period (documenting average or 'normal' thermal conditions at the geographical location of the capture site for the 1 April–31 July period). Because species are expected to be adapted to local thermal conditions (cf., Bergmann's rule; Ashton, 2002), we analysed the interannual variation in body size in response to temperature variations using annual local temperature anomalies (instead of raw temperatures). Local temperature anomalies (denoted as TA_{st}) were computed for each site as the difference between T_S and $T_{S.Y}$. Analysing the effects of temperature anomaly and local average temperature simultaneously enables the respective effects of temporal ($T_{S.Y}$) and spatial (T_S) variations in thermal conditions on body size to be disentangled. Temperature anomaly and local average temperature were largely uncorrelated (Pearson's r = .007).

2.4 | Statistical analysis

Using linear mixed models (MCMCglmm; Hadfield, 2010), we assessed the effects of yearly temperature anomalies TA_{st} on the juvenile body sizes of our study species, and their interaction with the local average temperature T_s (to assess whether the effect of TA_{st} varied along the species' thermal ranges). We used uniform priors, with a burn-in of 20,000 iterations, followed by an additional 100,000 iterations for which posteriors were sampled with an interval of 100.

We first built a null model (Model 0 in Table 1) that included only adjustment variables, to verify that the inclusion of temperature variables enhanced the explanatory power. The null model and all the following models (Table 1) accounted for the following sources of variation in wing length: (a) differences in mean size between species (fixed, factorial *Species* effect), (b) species-specific post-fledgling growth throughout the season, using log-transformed Julian date [denoted as *log(Date)*] as a fixed, linear effect in interaction with species (Dubos et al., 2018), (c) temperature-driven spatial differences between sites (e.g., Bergmann's rule) using a fixed, linear effect of local average temperature T_s, and (d) species-specific dependence on local average temperature (fixed, factorial *Species* × T_s interaction). This interaction term is justified by the fact that species may intrinsically respond differently to temperature (Ashton, 2002), or may respond differently because the thermal ranges of the study species differ (e.g., for some species, French populations are located at the core of the thermal range, whereas for other species, French populations are closer to the species hot limit; Jarema, Samson, McGill, & Murray, 2009). Consistent (e) between-observer, (f) between-site and (g) residual between-year variations were accounted for by random terms. Finally, (h) comparative tests across species accounted for phylogenetic relatedness using pairwise phylogenetic distances. We extracted a set of 100 generated phylogenetic trees from Jetz et al., (2014) and integrated these using the 'pedigree' argument of the MCMCglmm function, which allows the portion of body size variation due to additive genetic variance to be disentangled from other sources of variance.

Then we built a set of models to assess the statistical support for our prediction. We first considered the dependence of wing length on temperature anomalies (linear, additive effect of TA_{st}, Model 1). Then we accounted for the possibility that species respond differently (Jiguet et al., 2006) by adding the TA_{st} × *Species* interaction term (Model 2). The dependence on temperature anomaly could differ along the observed thermal gradient; this was allowed for by adding the TA_{st} × T_s interaction term to Model 1 (Model 3). In addition, this hypothesis was assessed with a model that also accounted for the possibility that species response to TA_{st} differed between species (i.e., adding the TA_{st} × T_s interaction to Model 2, resulting in Model 4). Eventually, we allowed for species-specific relationships between temperature anomaly TA_{st} and local average temperature T_s by adding a third-order interaction term between the effects of TA_{st}, T_s and species (Model 5). This model allows for a different direction and/or strength of both temperature effects between species. Model 5 results in the following formula:

$$\text{Wing length}_{isot} \sim \alpha_i + \beta_{i1}.\log(\text{Date}) + \beta_{i2}.\text{T}_s$$
$$+\beta_3.\text{TA}_{st} + \beta_{i3}.\text{TA}_{st} + \beta_4.(\text{TA}_{st} \times \text{T}_s) + \beta_{i4}.(\text{TA}_{st} \times \text{T}_s) + \varepsilon_s + \varepsilon_o + \varepsilon_t + \varepsilon_{isot}$$

where α_i is the average size of species *i* (intercept), β_{i1} is the slope for the effect of log-transformed Date for species *i*, β_{i2} is the species-specific slope for the effect of local average temperature T_s, β_3 is the slope for the additive effect of temperature anomaly TA_{st}, β_{i3} is the species-specific deviation from β_3 (species interaction term), β_4 is the slope for the interaction between the effects of temperature anomaly TA_{st} and local average temperature T_s, β_{i4} is the species-specific deviation from β_4 (species interaction term), ε_s, ε_o and ε_t hold respectively for the random terms for site, observer and year effects, and ε_{isot} is the residual variation.

The stepwise examination of predictions relied on the comparison of the six aforementioned models (Table 1), ranked on the basis of the deviance information criterion (DIC, a Bayesian version of the Akaike information criterion; Spiegelhalter, Best, & Carlin, 2002). The model with the lowest value of DIC is considered to represent the best trade-off between parsimony and fit of the model to the data. Each model was fitted using 100 different phylogenetic trees, so that the average of all posteriors accounted for between-species phylogenetic dependence. All statistical analyses were performed using R version 3.3.0 (R Core Team, 2016).

TABLE 1 Set of models used to assess the relationship between juvenile wing length, local temperature anomaly, local average temperature and species identity. The lowest deviance information criterion (DIC) indicates the 'best' model (in bold), and ΔDIC is the DIC difference with the best model. TA_{st} holds for the local temperature anomalies for a site *s* in year *t*, during the breeding season. T_s is the average temperature for a site *s* across the 2000–2014 breeding seasons. All models included the same adjustment variables (see text). Based on DIC, Models 4 and 5 received similar statistical support

Model	Model description	DIC	ΔDIC
M0	Species + T_s + Species × T_s + other adjustment var. (see text)	150,879	28
M1	M0 + TA_{st}	150,878	27
M2	M1 + TA_{st} × Species	150,860	9
M3	M1 + TA_{st} × T_s	150,869	18
M4	M2 + TA_{st} × T_s	**150,851**	**2**
M5	M4 + TA_{st} × $T_{s\,\times}$ Species	**150,849**	**0**

3 | RESULTS

The body size response to temperature anomaly TA_{st} differed between species. The model allowing for species-specific responses was better supported than the model assuming an additive response, common to all species (Model 2, Table 1). In accordance with our prediction, this response to TA_{st} varied along thermal gradients (Models 4 and 5 received the highest statistical support; Table 1). The effect of temperature anomaly on body size depends on the local average temperature.

On average across species, at an intermediate site (i.e., for a mean local average temperature T_s = 15.05 °C) the higher the temperature anomaly, the longer the wing length (+ 0.9 mm per °C anomaly; Model 3 in Table S2). But, the warmer the site (local average temperature, T_s), the lower the effect of temperature anomaly on wing length (for a + 1 °C increase in local average temperature, the effect deceases by 0.052 mm per °C anomaly; Model 4 in Table S2). At the hottest sites, the effect of temperature anomaly was even reversed, with a potential decrease in wing length in the warmest years (Figure 2). The nature of this 'temperature anomaly - by - local average temperature' interaction may differ between species, but these differences seem to be of minor importance in our dataset (as ΔDIC is only 2 between Models 4 and 5; Tables 1 and S2). When plotting estimates for the interactive effects of TA_{st} and T_s per species (Figures 3 and S2), the response of body size is largely similar across species. Relying on Model 5, the three species showing a significantly positive effect of temperature anomaly at the coolest sites showed a significant interactive effect with local average temperature (i.e., Eurasian blackcap, long-tailed tit and great tit; Table S2). At the coolest sites (between 8.37 and 13.9 °C depending on the species), body size increased significantly in warmer years for these species (respectively, by 0.86, 1.71 and 0.54 mm per °C; Table 2). The temperature anomaly effect decreased when the local average temperature increased: for a + 1 °C increase in local average temperature, the wing length of Eurasian blackcaps decreased by −0.072 mm per °C of anomaly, −0.324 mm per °C for long-tailed tits, and −0.072 mm per °C for great tits (Table S2). This effect decreased enough to become negative for two species at the warmest sites (i.e., long-tailed tit: −1.06 mm per °C of anomaly; European blackcap: −0.29 mm per °C of anomaly at a site with an average temperature of 18.2 °C; Table 2; Figures S3 and S4). For these two species, the 'tipping-point' of local temperature, that is, at which the sign of the effect of temperature anomaly changes, was located between the core and the hot edge of their respective thermal range (respectively for thermal coordinates of 0.77 and 0.70). For the great tit, the effect of temperature anomaly became null toward the hot edge of its thermal range (Table 2).

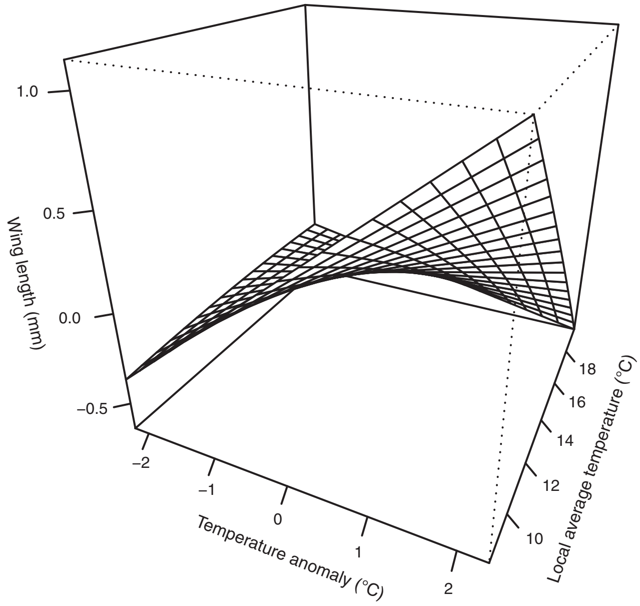

FIGURE 2 Residual response of average juvenile wing length to temperature anomaly along a gradient in average local temperature, for nine breeding songbird species from France. Predicted values were obtained from MCMCglmm (Model 3, see text and Table 1). Local average temperature is the mean spring temperature of a given site for the period 2000–2014. Wing length was centred on the mean value per species. Species-specific predicted values are shown in the Supporting Information (Figure S3)

4 | DISCUSSION

As expected in Figure 1, the response of body size to temperature anomaly depended on the position of populations within the species' thermal range. At the coldest sites, juveniles were larger in warmer years, but the size of those born at the warmest sites did not depend on spring temperature anomalies (or even declined in hot springs for some species).

The positive effect of temperature anomalies in cold regions may be related to both direct effects, through changes in thermoregulatory mechanisms, and indirect effects, through changes in food availability (Yom-Tov & Geffen, 2011). Warmer years induce a reduction of the cost of body heat maintenance in cool areas, enabling a higher energetic allocation to body growth (Gillooly et al., 2001). An alternative, non-exclusive hypothesis is that warming may also increase net primary production, thus improving invertebrate abundance (Dubos et al., 2018; Yom-Tov & Geffen, 2011). In the present study, all study species are insectivorous during spring. Higher invertebrate abundance in some years may have enhanced juvenile protein intake, allowing them to reach larger fledgling sizes at the coolest sites (Lindström, 1999).

The opposite effect, found for two species (long-tailed tits and Eurasian blackcaps) at the warmest sites, is consistent with the application of Bergmann's rule to climate warming (Gardner et al., 2011). The consequences of a local increase in temperature on individual fitness were shown to differ between species of different latitudes in a previous study (Deutsch et al., 2008). At low latitudes, warming has more deleterious consequences on fitness than at higher latitudes. This is due to the fact that, at low latitudes (e.g., tropical), species live close to the upper boundary of their thermal tolerance, while high latitude species live farther from that lethal limit (Deutsch et al., 2008; Tewksbury et al., 2008). This process seems to apply at the intraspecific level, within a species' range. The negative effect of temperature anomaly on juvenile body size may be explained by two mechanisms. This may be the result of (a) a plastic response to environmental change on growth rates (Teplitsky & Millien, 2014). Hotter years in warm areas would bring growing juveniles into suboptimal thermal conditions for juvenile growth (Mertens, 1977; Rodríguez & Barba, 2016), which would result in smaller individuals. Size declines in hotter years could also be the result of (b) size-dependent mortality: the largest individuals would suffer the most from hyperthermia, and be more likely to die in warm years. However, lethal temperatures are rarely reached in temperate regions (mean number of days >35 °C = 0.13 ± 0.28 *SD* days per spring at our study

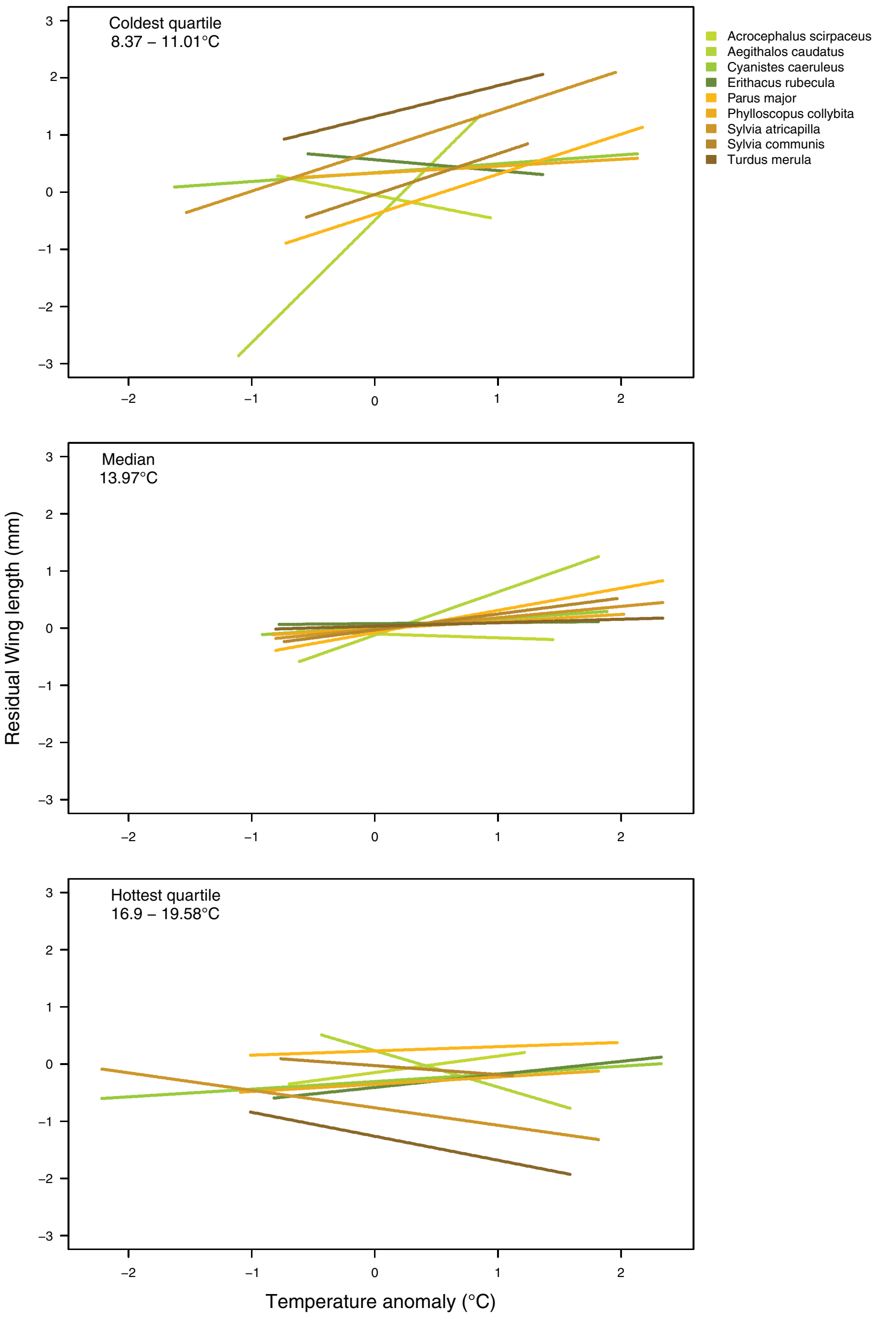

FIGURE 3 Species-specific response of juvenile wing length to spring temperature anomaly, separated into three quantiles of local average temperature, for nine breeding songbird species from France. Predicted values were obtained from MCMCglmm (Model 5, Table 1). Wing length was centred on species means. Local average temperature is the mean spring temperature of a given site for the period 2000–2014. Coldest quartile: average response at the 25% coldest sites (*n* = 9); median quartiles: average response at the 25–75% intermediate sites (*n* = 180); hottest quartile: average response at the 75% hottest sites (*n* = 15) [Colour figure can be viewed at wileyonlinelibrary.com]

sites). Hence, from the present dataset, even at the hottest sites, a higher mortality level for larger individuals in hot years would not be expected in France. Most studies attempting to find evidence of selection for smaller size failed to do so, or found the opposite pattern (Dunn, Hamer, & Benton, 2016). The hypothesis of a cold constraint release for juvenile growth in hotter years is therefore the most likely in temperate climates. Our results are consistent with Danner and Greenberg (2015), suggesting that in temperate species, morphology is constrained by cold toward the coldest edge of their distribution range – and potentially across most of their temperate distribution range (i.e., not all individuals achieve optimal body size) – whereas at the hottest edge, heat (or drought-driven food shortage) would be the predominating constraint. An additional hypothesis is that very high temperatures could reduce parental foraging efficiency, for example, due to physiological stress (hyperthermia, water loss) enhanced

TABLE 2 Estimates of temperature anomaly (TA_{st}) at the observed coldest ($T_s$min) and hottest ($T_s$max) species-specific study sites, and the local average temperature (T_s) where the temperature anomaly effect is predicted to reverse (i.e., is null). Numbers in parentheses indicate the corresponding thermal coordinate (a value of 0 represents the coldest sites where the species can be present, and 1 represents the hottest sites; Table S1). Predicted values were obtained from MCMCglmm posterior estimates (Model 5 in Table 1) and accounted for phylogenetic relatedness (species are sorted accordingly)

		TA_{st} effect at T_s min			TA_{st} effect at T_s max		
Species	T_s min (°C)	Slope (mm/°C)	% of wing length	T_s max (°C)	Slope (mm/°C)	% of wing length	T_s (°C) at null *TA* effect
Parus major	13.2	0.54	1.0	19.6	−0.02	−0.3	20.9 (1.00)
Parus caeruleus	11.0	−0.25	−0.8	19.6	0.22	0.2	–
Acrocephalus scirpaceus	8.4	−0.13	−0.7	18.8	0.39	0.1	–
Sylvia atricapilla	8.5	0.86	0.5	18.2	−0.29	−0.3	15.1 (.70)
Sylvia communis	12.0	0.28	0.7	19.6	−0.15	−0.3	15.1 (.79)
Phylloscopus collybita	11.4	0.12	0.8	18.2	0.12	0.2	–
Aegithalos caudatus	8.4	1.71	0.9	18.2	−1.06	−0.1	16.4 (.77)
Turdus merula	13.9	0.68	0.3	18.2	−0.39	−0.4	12.3 (.60)
Erithacus rubecula	8.4	0.16	0.6	18.0	0.13	0.2	–

by reduced invertebrate activity (Cunningham, Martin, Hojem, & Hockey, 2013; Geiser, Arlettaz, & Schaub, 2008). Lower parental feeding frequency could affect offspring growth rate, and result in smaller fledglings (Searcy, Peters, & Nowicki, 2004).

The indirect effects of temperature anomaly on ecosystem production – and therefore food availability—at the hottest sites may also differ from the coldest sites. In semi-arid environments, net primary production depends on precipitation to a greater extent than temperature (e.g., Holmgren et al., 2016). This may apply to the French Mediterranean region, as both climates are similar (see www.worldclimate.com). Hence, it is unlikely that temperature response is driven by changes in net primary production at the warmest study sites, which may explain the decreasing effect of temperature anomaly toward the hottest sites. Another hypothesis is that, because temperature change can impact food web structures (e.g., Edeline, Lacroix, Delire, Poulet, & Legendre, 2013), a differential effect may be the consequence of differing changes in the biotic environment. The effect of temperature change on body size, through changes in food availability in ecosystems, may therefore depend on the regional climate and ecosystems, regardless of the population's position within the species' thermal range. These antagonistic or synergistic effects of local temperature, precipitation and ecosystem structures on individual body size deserve to be investigated in future research.

Body size response to warming may depend on the average climate under which the local population evolved, as found for temporal trends in population size (Jiguet et al., 2010). The consequences of climate warming on populations are often more deleterious at the hot edge of a species' distribution, while it can be favourable at the cold edge (Hickling, Roy, Hill, Fox, & Thomas, 2006; Leroy et al., 2014; Parmesan & Yohe, 2003), with a linear graded response in between (Jiguet et al., 2010). Although the present analysis included a relatively wide range of thermal conditions (> 11 °C), the number of sites in cold and hot regions was limited (Figure S1). We used species for which the distribution edges are not (or rarely) included in our study area (Figure S2). Despite species response to warming which may be stronger at the edges of their distribution range (Jarema et al., 2009), we still detected a differential response along a fragment of their range. Moreover, while responses to warming are expected to be greater in thermal specialists (i.e., species with a narrow thermal range compared to other Palaearctic species; Jiguet et al., 2006), our results were obtained from species that are mostly thermal generalists (i.e., with a wide thermal range; Table S1). This suggests that differential effects of temperature change on body size may apply to a wide range of species (including thermal generalists), which is consistent with results obtained for population trends (Jiguet et al., 2010). In spite of geographical and taxonomic limits, the pattern revealed is the one expected theoretically (cf. abundance, phenology patterns), and we provide the first evidence for a structured effect of temperature on body size. Studies performed at a large geographical scale, aiming at testing the effect of temperature variation on body size – while assuming a uniform effect – may therefore fail to detect an effect of temperature change because it may be blurred by opposing effects between sites.

The estimated effect sizes for the influence of temperature anomaly on body size are small, ranging from −0.8 to 1.0% of species' mean wing length per C of annual anomaly. Compared to spatial effects of temperature (i.e., local average temperature; cf. Bergmann's rule), these effects sizes were of similar magnitude (−0.23 to 0.16% per C; Table S2). In other studies focussing on temporal variation in bird size, the effect of mean temperature of the breeding period was about 1% of the juvenile wing length in Australia, and the effect of summer temperature ranged between −0.63 and 0.15% per C in eastern North America (Collins et al., 2017a). Recently, Dubos et al. (2018) reported that, when analysing additive effects of annual weather on wing length across sites and species, they could explain 5% of the total variance in juvenile wing length at best, that is, the additive and species-specific variation between years.

All the remaining variance actually corresponds to site-specific annual variations (7%) or site- and species-specific annual variations (88%). Hence, we acknowledge that effect sizes are indeed small, and that this questions the biological relevance of the corresponding size changes. This concern about small size effects applies to most existing studies on short-term body size changes, and is a recurrent issue in ecology (Møller & Jennions, 2002). Given the multiple determinants of body size, it even appears obvious that body size cannot drastically change between years and generations. Hence, whatever the influence of the environment on juvenile body size, it will always be restricted to a narrow range of change of average size, beyond which other compensatory mechanisms start to come into play (e.g., offspring mortality, early termination of growth). We are not aware of a statistical framework, applicable to existing data, that would allow objective qualification of the biological relevance of the observed, statistically robust effects of temperature on wing length.

In the present study, we focussed on spring temperatures because this corresponds to the period of body growth, as body size has been shown to be mainly driven by the conditions during this period (Yom-Tov & Geffen, 2011), and because in songbirds, body growth ends soon after fledging (some weeks). However, high temperatures may drive size-dependent mortality in juveniles, as they are more exposed to hypo- or hypertheremia than their parents (Mertens, 1977). In addition, size-dependent mortality can also affect adults, and mortality can occur at later stages of individuals' lives (i.e., carry-over effects; van de Pol & Cockburn, 2011). Getting the full picture of body size responses to temperature will require investigation of its effects during other parts of the year (e.g., winter, when bird mortality is the highest in temperate climates; Van Balen, 1980), at different time-scales (Kruuk et al., 2015), and include assessments of size-dependent mortality (e.g., using mark–recapture approaches).

To conclude, the differential effect of climate warming along species ranges already found in species distributions (Hickling et al., 2006), phenological shifts (Both & te Marvelde, 2007) and population trends (Jiguet et al., 2010) also applies to body size. We predict that climate warming will induce body size increases (up to optimal body size) more frequently at the cold edges of species distribution ranges, and body size declines will be more likely at the hot edges. In France, the impact of warming on avian population dynamics may impact body size negatively at the warmest sites, corresponding to the Mediterranean region, where species (including our study species) live closer to the upper boundary of their thermal tolerance (Jiguet et al., 2010). As individual fitness is often size-dependent, with the largest surviving and/or reproducing better (Lindström, 1999; Ronget et al., 2017), it is to be feared that size decline may impact populations negatively. To assess the robustness and generality of our conclusions, future studies should investigate the synergistic effects of local temperature anomalies (weather fluctuations) and local average temperatures (climate) on body size across a larger number of species (including a broader spectrum of life-history traits, and particularly more thermal specialists), and across a broader climatic range, to include the entire thermal ranges of the species studied. Another challenge for future studies on the link between body size and temperature fluctuations will be to sort out the proximate mechanisms at play (e.g., ontogeny versus mortality and thermal versus trophic pressure).

ACKNOWLEDGEMENTS

This study was made possible thanks to the 382 ringers that voluntarily monitor birds as part of the *STOC Capture* scheme (Appendix S2), and to the continuous support of Muséum National d'Histoire Naturelle, CNRS and Ministry of Environment. ND was funded by LabEx BCDiv. We acknowledge the E-OBS dataset from the EU-FP6 project ENSEMBLES (https://ensembles-eu.metoffice.com) and the data providers in the ECA&D project (https://www.ecad.eu). We thank Manon Ghislain for her help with data preparation, and Vincent Devictor, Romain Julliard, Boris Leroy, Alexandre Robert and Céline Teplitsky for useful discussions. We are very grateful to Liam Bailey, Jacob Socolar and Shai Meiri for their helpful comments, which improved the manuscript.

DATA ACCESSIBILITY

The dataset used in this analysis is available as an R object in the Supporting Information.

ORCID

Nicolas Dubos http://orcid.org/0000-0002-1224-2598

REFERENCES

Allen, J. A. (1877). The influence of physical conditions in the genesis of species. *Radical Review*, *1*, 108–140.

Ashton, K. G. (2002). Patterns of within-species body size variation of birds: Strong evidence for Bergmann's rule. *Global Ecology and Biogeography*, *11*, 505–523.

Bale, J. S., Masters, G. J., Hodkinson, I. D., Awmack, C., Bezemer, T. M., Brown, V. K., … Whittaker, J. B. (2002). Herbivory in global climate change research: Direct effects of rising temperature on insect herbivores. *Global Change Biology*, *8*, 1–16. https://doi.org/10.1046/j.1365-2486.2002.00451.x

Bergmann, C. (1847). *Uber die Verhaltnisse der Warmeokonomie der Thiere zu ihrer Grosse*, Göttingen. Göttinger.

Björklund, M., Borras, A., Cabrera, J., & Senar, J. C. (2014). Increase in body size is correlated to warmer winters in a passerine bird as inferred from time series data. *Ecology and Evolution*, 59–72.

Both, C., & te Marvelde, L. (2007). Climate change and timing of avian breeding and migration throughout Europe. *Climate Research*, *35*, 93–105. https://doi.org/10.3354/cr00716

Collins, M. D., Relyea, G. E., Blustein, E. C., & Badami, S. M. (2017a). Heterogeneous changes in avian body size across and within species. *Journal of Ornithology*, *158*, 39–52. https://doi.org/10.1007/s10336-016-1391-x

Collins, M. D., Relyea, G. E., Blustein, E. C.& Badami, M. (2017b). Neotropical migrants exhibit variable body-size changes over time and space. *Northeastern Naturalist* , *24*, 82–96.

Cunningham, S. J., Martin, R. O., Hojem, C. L., & Hockey, P. A. R. (2013). Temperatures in excess of critical thresholds threaten nestling growth and survival in a rapidly-warming arid savanna: A study of common fiscals. *PLoS ONE*, *8*(9), e74613.

Danner, R. M., & Greenberg, R. (2015). A critical season approach to Allen's rule: Bill size declines with winter temperature in a cold temperate environment. *Journal of Biogeography*, *42*, 114–120. https://doi.org/10.1111/jbi.12389

Dawson, R. D., Lawrie, C. C., & O'Brien, E. L. (2005). The importance of microclimate variation in determining size, growth and survival of avian offspring: Experimental evidence from a cavity nesting passerine. *Oecologia*, *144*, 499–507.

Dehorter, O., & CRBPO. (2017). Bird ringing and movement database for France.

Deutsch, C. A., Tewksbury, J. J., Huey, R. B., Sheldon, K. S., Ghalambor, C. K., Haak, D. C., & Martin, P. R. (2008). Impacts of climate warming on terrestrial ectotherms across latitude. *Proceedings of the National Academy of Sciences USA*, *105*, 6668–6672. https://doi.org/10.1073/pnas.0709472105

Dubos, N., Viol, I. L., Robert, A., Teplitsky, C., Ghislain, M., Dehorter, O., … Henry, P.-Y. (2018). Disentangling the effects of spring anomalies in climate and net primary production on body size of temperate songbirds. *Ecography*, *41*, 1319–1330. https://doi.org/10.1111/ecog.03413

Dunn, J. C., Hamer, K. C., & Benton, T. I. M. G. (2016). *Dynamics of phenotypic change: wing length declines in a resident farmland passerine despite survival advantage of longer wings*. *IBIS*, *159*, 152–157.

Edeline, E., Lacroix, G., Delire, C., Poulet, N., & Legendre, S. (2013). Ecological emergence of thermal clines in body size. *Global Change Biology*, *19*, 3062–3068. https://doi.org/10.1111/gcb.12299

Eglington, S. M., Julliard, R., Gargallo, G., van der Jeugd, H. P., Pearce-Higgins, J. W., Baillie, S. R., & Robinson, R. A. (2015). Latitudinal gradients in the productivity of European migrant warblers have not shifted northwards during a period of climate change. *Global Ecology and Biogeography*, *24*, 427–436. https://doi.org/10.1111/geb.12267

Garcia, R. A., Cabeza, M., Rahbek, C., & Araújo, M. B. (2014). Multiple dimensions of climate change and their implications for biodiversity, *Science*, *344*, 1247579.

Gardner, J. L., Amano, T., Mackey, B. G., Sutherland, W. J., Clayton, M., & Peters, A. (2014). Dynamic size responses to climate change: Prevailing effects of rising temperature drive long-term body size increases in a semi-arid passerine. *Global Change Biology*, *20*, 2062–2075.

Gardner, J. L., Peters, A., Kearney, M. R., Joseph, L., & Heinsohn, R. (2011). Declining body size: A third universal response to warming? *Trends in Ecology and Evolution*, *26*, 285–291. https://doi.org/10.1016/j.tree.2011.03.005

Gardner, J. L., Rowley, E., Rebeira, P. D., Rebeira, A. D., & Brouwer, L. (2017). Effects of extreme weather on two sympatric Australian passerine bird species. *Philosophical Transactions of the Royal Society B: Biological Sciences*, *372*, 20160148. https://doi.org/10.1098/rstb.2016.0148

Geiser, S., Arlettaz, R., & Schaub, M. (2008). Impact of weather variation on feeding behaviour, nestling growth and brood survival in Wrynecks *Jynx torquilla*. *Journal of Ornithology*, *149*, 597–606. https://doi.org/10.1007/s10336-008-0305-y

Gillooly, J. F., Brown, J. H., West, G. B., Savage, V. M., & Charnov, L. (2001). Effects of size and temperature on metabolic rate. *Science*, *293*, 2248–2251.

Gosler, A. G., Greenwood, J. J. D., Baker, J. K., … N. C. (1998). The field determination of body size and condition in passerines: A report to the British Ringing Committee. *Bird Study*, *45*, 92–103. https://doi.org/10.1080/00063659809461082

Greenberg, R., Cadena, V., Danner, R. M., & Tattersall, G. (2012). Heat loss may explain bill size differences between birds occupying different habitats. *PLoS ONE*, *7*, 1–9.

Hadfield, J. D. (2010). MCMC methods for multi-response generalized linear mixed models: The MCMCglmm R package. *Journal of Statistical Software*, *33*, 1–22.

Haylock, M. R., Hofstra, N., Tank, A. K., Klok, E. J., Jones, P. D., & … M. (2008). A European daily high-resolution gridded data set of surface temperature and precipitation for 1950–2006. *Journal of Geophysical Research*, *113*, D20119. https://doi.org/10.1029/2008JD010201

Hickling, R., Roy, D. B., Hill, J. K., Fox, R., & Thomas, C. D. (2006). The distributions of a wide range of taxonomic groups are expanding polewards. *Global Change Biology*, *12*, 450–455. https://doi.org/10.1111/j.1365-2486.2006.01116.x

Holmgren, M., Stapp, P., Dickman, C. R., Gracia, C., Graham, S., Gutiérrez, J. R., … Squeo, F. A. (2016). Extreme climatic events shape arid and semiarid ecosystems. *Frontiers in Ecology and the Environment*, *4*, 87–95.

Husby, A., Hille, S. M., & Visser, M. E. (2011). Testing mechanisms of Bergmann's rule: Phenotypic decline but no genetic change in body size in three passerine bird populations. *The American Naturalist*, *178*, 202–213. https://doi.org/10.1086/660834

Jarema, J., Samson, J., McGill, B. I., & Murray, M. H. (2009). Variation in abundance across a species' range predicts climate change responses in the range interior will exceed those at the edge: A case study with North American beaver. *Global Change Biology*, *15*, 508–522.

Jetz, W., Thomas, G. H., Joy, J. B., Redding, D. W., Hartmann, K., & Mooers, A. O. (2014). Global distribution and conservation of evolutionary distinctness in birds. *Current Biology*, *24*, 919–930. https://doi.org/10.1016/j.cub.2014.03.011

Jiguet, F., Devictor, V., Ottvall, R., Van Turnhout, C., Van der Jeugd, H., & Lindström, A. (2010). Bird population trends are linearly affected by climate change along species thermal ranges. *Proceedings of the Royal Society B: Biological Sciences*, *277*, 3601–3608. https://doi.org/10.1098/rspb.2010.0796

Jiguet, F., Julliard, R., Thomas, C. D., Dehorter, O., Newson, S. E., & Couvet, D. (2006). Thermal range predicts bird population resilience to extreme high temperatures. *Ecology Letters*, *9*, 1321–1330. https://doi.org/10.1111/j.1461-0248.2006.00986.x

Kendeigh, C. (1969). Tolerance of cold and Bergmann's Rule. *The Auk*, *86*, 13–25. https://doi.org/10.2307/4083537

Khaliq, I., Hof, C., Prinzinger, R., Böhning-Gaese, K., & Pfenninger, M. (2014). Global variation in thermal tolerances and vulnerability of endotherms to climate change. *Proceedings of the Royal Society B: Biological Sciences*, *281*, 20141097. https://doi.org/10.1098/rspb.2014.1097

Kruuk, L. E. B., Osmond, H. L., & Cockburn, A. (2015). Contrasting effects of climate on juvenile body size in a Southern Hemisphere passerine bird. *Global Change Biology*, *21*, 2929–2941. https://doi.org/10.1111/gcb.12926

Leroy, B., Bellard, C., Dubos, N., Colliot, A., Vasseur, M., Courtial, C., … Ysnel, F. (2014). Forecasted climate and land use changes, and protected areas: The contrasting case of spiders. *Diversity and Distributions*, *20*, 686–697. https://doi.org/10.1111/ddi.12191

Lindström, J. (1999). Early development and fitness in birds and mammals. *Trends in Ecology and Evolution*, *14*, 343–348. https://doi.org/10.1016/S0169-5347(99)01639-0

McKechnie, A. E., & Wolf, B. O. (2010). Climate change increases the likelihood of catastrophic avian mortality events during extreme heat waves. *Biology Letters*, *6*, 253–256. https://doi.org/10.1098/rsbl.2009.0702

Meiri, S., Guy, D., Dayan, T., & Simberloff, D. (2009). Global change and carnivore body size: Data are stasis. *Global Ecology and Biogeography*, *18*, 240–247. https://doi.org/10.1111/j.1466-8238.2008.00437.x

Mertens, J. A. L. (1977). Thermal conditions for successful breeding in great tits (*Parus major* L.) - I. Relation of growth and development of temperature regulation in nestling great tits. *Oecologia*, *28*, 1–29. https://doi.org/10.1007/BF00346834

Møller, A. P., & Jennions, M. D. (2002). How much variance can be explained by ecologists and evolutionary biologists? *Oecologia*, *132*, 492–500. https://doi.org/10.1007/s00442-002-0952-2

Parmesan, C., & Yohe, G. (2003). A globally coherent fingerprint of climate change impacts across natural systems. *Nature*, *421*, 37–42. https://doi.org/10.1038/nature01286

Peel, M. C., Finlayson, B. L., & McMahon, T. A. (2007). Updated world map of the Köppen-Geiger climate classification. *Hydrology and Earth System Sciences Discussions*, *4*, 439–473. https://doi.org/10.5194/hessd-4-439-2007

Pérez, J. H., Krause, J. S., Chmura, H. E., Bowman, S., McGuigan, M., Asmus, A. L., … Wingfield, J. C. (2016). Nestling growth rates in relation to food abundance and weather in the Arctic. *The Auk*, *133*, 261–272. https://doi.org/10.1642/AUK-15-111.1

R Core Team (2016). R: A language and environment for statistical computing. R foundation for statistical computing.

Robinson, R. A., Julliard, R., & Saracco, J. F. (2009). Constant effort: Studying avian population processes using standardised ringing. *Ringing & Migration*, *24*, 199–204.

Rodríguez, S., & Barba, E. (2016). Nestling growth is impaired by heat stress: An experimental study in a mediterranean great tit population. *Zoological Studies*, *55*, 40.

Ronget, V., Gaillard, J. M., Coulson, T., Garratt, M., Gueyffier, F., Lega, J. C., & Lemaître, J. F. (2017). Causes and consequences of variation in offspring body mass: Meta-analyses in birds and mammals. *Biological Reviews*, *93*, 1–27. https://doi.org/10.1111/brv.12329

Salewski, V., Hochachka, W. M., & Fiedler, W. (2010). Global warming and Bergmann's rule: Do central European passerines adjust their body size to rising temperatures? *Oecologia*, *162*, 247–260. https://doi.org/10.1007/s00442-009-1446-2

Searcy, W. A., Peters, S., & Nowicki, S. (2004). Effects of early nutrition on growth rate and adult size in song sparrows *Melospiza melodia*. *Journal of Avian Biology*, *35*, 269–279.

Socolar, J. B., Epanchin, P. N., Beissinger, S. R., & Tingley, M. W. (2017). Phenological shifts conserve thermal niches in North American birds and reshape expectations for climate-driven range shifts. *Proceedings of the National Academy of Sciences USA*, *114*, 12976–12981. https://doi.org/10.1073/pnas.1705897114

Spiegelhalter, D. J., Best, N. G., & Carlin, B. P. (2002). Bayesian measures of model complexity and fit. *Journal of the Royal Statistical Society*, *64*, 583–639.

Svensson, L. (1992). *Identification guide to European passerines*. Stockholm: Märstatryc.

Teplitsky, C., & Millien, V. (2014). Climate warming and Bergmann's rule through time: Is there any evidence? *Evolutionary Applications*, *7*, 156–168. https://doi.org/10.1111/eva.12129

Tewksbury, J. J., Huey, R. B., & Deutsch, C. A. (2008). Putting the heat on tropical animals the scale of prediction. *Science*, *320*, 1296–1297.

Van Balen, J. H. (1980). Population fluctuations of the great tit and feeding conditions in winter. *Ardea*, *68*, 143–164.

van de Pol, M., & Cockburn, A. (2011). Identifying the critical climatic time window that affects trait expression. *The American Naturalist*, *177*, 698–707. https://doi.org/10.1086/659101

Yom-Tov, Y., & Geffen, E. (2011). Recent spatial and temporal changes in body size of terrestrial vertebrates: Probable causes and pitfalls. *Biological Reviews*, *86*, 531–541. https://doi.org/10.1111/j.1469-185X.2010.00168.x

BIOSKETCH

Nicolas Dubos is a researcher in macroecology, specializing in modelling species response to environmental change in temperate and tropical systems. This article was part of his Ph.D. at the Museum National d'Histoire Naturelle. His research teams focus on (a) biodiversity conservation, with a particular interest in bird ecology (CESCO), and (b) understanding the mechanisms underlying species responses to environmental change (MECADEV).

SUPPORTING INFORMATION

Additional supporting information may be found online in the Supporting Information section at the end of the article.

How to cite this article: Dubos N, Dehorter O, Henry P-Y, Le Viol I. Thermal constraints on body size depend on the population's position within the species' thermal range in temperate songbirds. *Global Ecol Biogeogr*. 2019;28:96–106. https://doi.org/10.1111/geb.12805

Thermal constraints on body size depend on the population position within the species' thermal range in temperate songbirds

Nicolas Dubos, Olivier Dehorter, Pierre-Yves Henry, Isabelle Le Viol

Supporting information

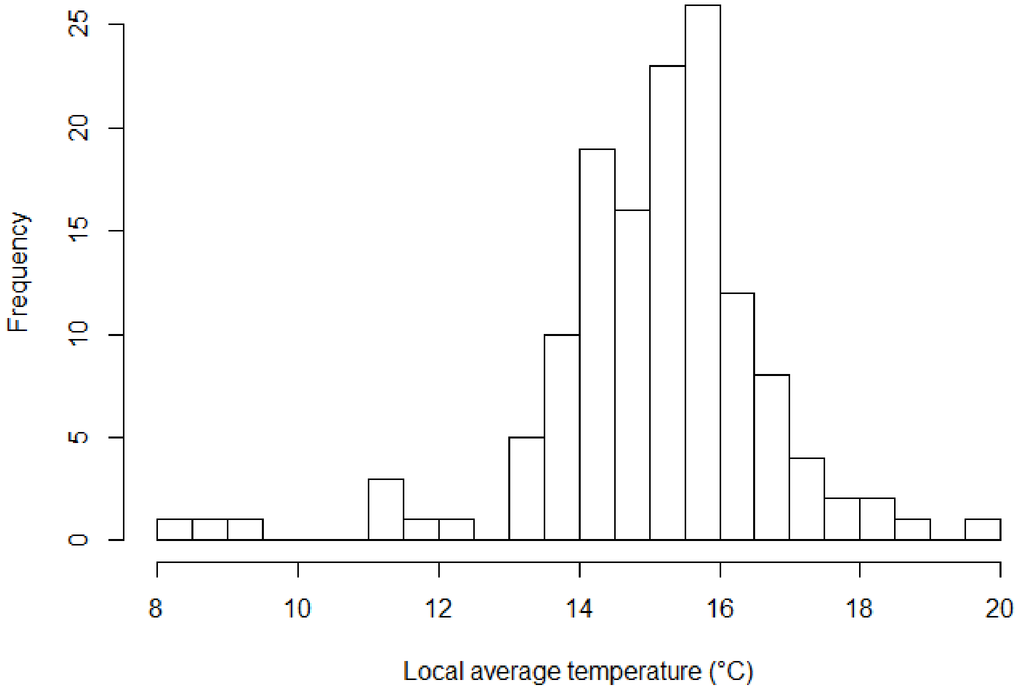

Fig. S1 Distribution of local average temperatures (i.e., mean temperature of a given site for the breeding period between 2000 and 2014) across 204 study sites in France.

Table S1 Species-specific thermal minimum (T min) and maximum (T max) at the European scale, minimum, maximum and range of local average temperatures (T_s) that are observed in the study area, and sample size for the nine studied species. The corresponding thermal coordinates are shown in parentheses (see Fig S1). Thermal coordinates of 0 and 1 respectively correspond to the coldest and the hottest site(s) of the European distribution area of the species (Jiguet *et al.* 2010). The 'Observed thermal range' corresponds to the difference in average temperatures between the hottest (Max. Average Temperature) and the coldest sites (Min. Average Temperature) that are included in the study area during the study period. The numbers in parentheses are the proportions of thermal ranges that are represented in the study area (observed thermal range) relative to species European thermal range. Average temperatures and thermal ranges were computed for the breeding season (1 April to 31 July), for studied sites, between 2000 and 2014.

Species	Species Tmin (°C)	Species Tmax (°C)	Min. Average Temperature (°C)	Max. Average Temperature (°C)	Observed thermal range (°C)	*n*
Acrocephalus scirpaceus	8.7	22.0	13.2 (0.33)	19.6 (0.82)	6.4 (0.48)	1105
Aegithalos caudatus	6.0	19.6	11.0 (0.37)	19.6 (1.00)	8.6 (0.64)	1217
Erithacus rubecula	4.6	19.6	8.4 (0.25)	18.8 (0.95)	10.4 (0.70)	5386
Cyanistes caeruleus	6.4	20.8	8.5 (0.15)	18.2 (0.82)	9.7 (0.67)	2251
Parus major	4.5	20.9	12.0 (0.46)	19.6 (0.92)	7.6 (0.47)	7115
Phylloscopus collybita	3.7	18.2	11.4 (0.55)	18.2 (1.00)	6.8 (0.48)	3667
Sylvia atricapilla	6.1	20.0	8.4 (0.16)	18.2 (0.86)	9.8 (0.71)	10191
Sylvia communis	6.8	20.3	13.9 (0.52)	18.2 (0.84)	4.2 (0.31)	1437
Turdus merula	5.4	21.8	8.4 (0.18)	18.0 (0.77)	9.7 (0.59)	1732

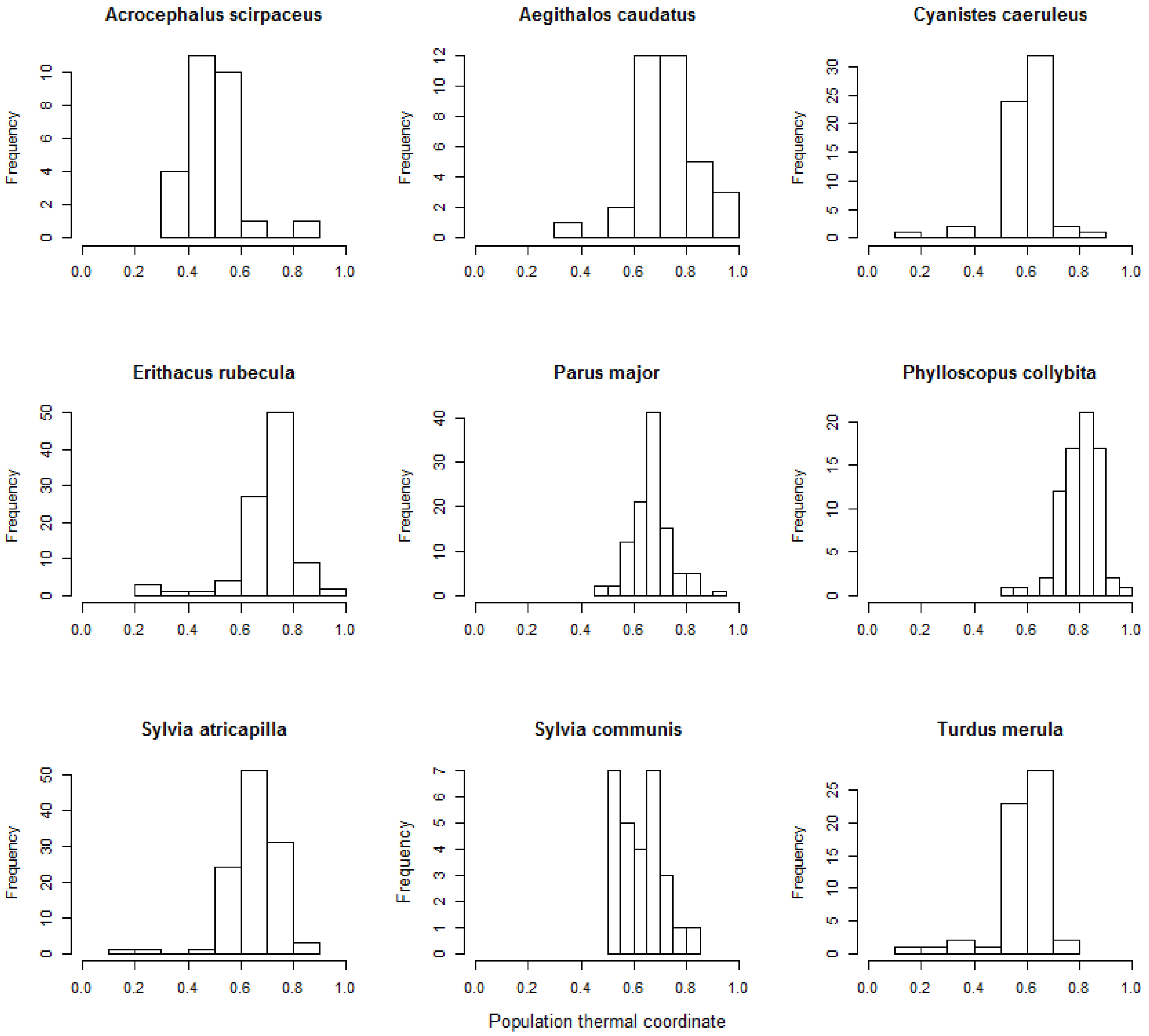

Fig. S2 Distribution of thermal coordinates (in number of sites) for the nine studied songbird species across 204 sites in France. A value of 0 corresponds to the coldest site of the species' distribution, while a value of 1 corresponds to the hottest sites (see Jiguet et al., 2010 for a detailed definition).

Table S2 Parameter estimates (Highest Posterior Density, HPD) for the relationship between wing length and local temperature anomaly (TA$_{st}$) according to local average temperature (T$_s$) for nine songbird species from France. Models were fitted, and estimates were obtained, using the MCMCglmm function. Local average temperature is the mean temperature of a given site for the breeding period between 2000 and 2014. Models accounted for phylogenetic relatedness (species are sorted accordingly). Effects of interest (corresponding to predictions) that are statistically supported are shown in bold. For the TA$_{st}$ effect, the estimate indicate overall size change (in mm) for a 1°C anomaly at a site with a mean T (and not for T = 0°, as this variable was centred here to avoid extrapolation). For the TA$_{st}$: T$_s$ interaction, the estimate indicates size change for a +1°C anomaly in local average temperature.

Fixed effect	Estimate	Lower 95% CI	Upper 95% CI	Effective sampling	pMCMC
Null model					
Parus major	53.590	50.260	56.880	10306	<1e-04
Parus caeruleus	53.870	48.660	59.510	10000	<1e-04
Acrocephalus scirpaceus	66.810	53.880	80.150	10312	<1e-04
Sylvia atricapilla	74.610	71.380	77.710	10762	<1e-04
Sylvia communis	59.780	50.780	68.890	10000	<1e-04
Phylloscopus collybita	53.890	49.150	58.940	10000	<1e-04
Aegithalos caudatus	55.950	48.980	62.750	10000	<1e-04
Turdus merula	116.000	110.400	121.800	11006	<1e-04
Erithacus rubecula	69.340	65.620	73.270	10000	<1e-04
Parus major : T$_s$	0.030	-0.061	0.123	10000	0.521
Parus caeruleus : T$_s$	-0.128	-0.250	-0.012	10000	0.035
Acrocephalus scirpaceus : T$_s$	0.106	-0.071	0.285	10000	0.246
Sylvia atricapilla : T$_s$	-0.134	-0.215	-0.053	10000	0.001
Sylvia communis : T$_s$	0.037	-0.129	0.199	10000	0.654
Phylloscopus collybita : T$_s$	-0.135	-0.249	-0.015	9614	0.021
Aegithalos caudatus : T$_s$	0.034	-0.124	0.176	10000	0.661
Turdus merula : T$_s$	-0.228	-0.351	-0.099	10000	0.000
Erithacus rubecula : T$_s$	-0.077	-0.154	0.000	10000	0.052
Parus major : log(Date)	3.964	3.395	4.520	9474	<1e-04
Parus caeruleus : log(Date)	2.533	1.577	3.542	10000	<1e-04
Acrocephalus scirpaceus : log(Date)	-0.746	-3.124	1.651	10000	0.550
Sylvia atricapilla : log(Date)	0.145	-0.396	0.702	10000	0.607
Sylvia communis : log(Date)	1.998	0.334	3.677	10000	0.019
Phylloscopus collybita : log(Date)	1.123	0.221	1.977	10000	0.013
Aegithalos caudatus : log(Date)	0.292	-0.980	1.559	10000	0.657
Turdus merula : log(Date)	2.557	1.501	3.593	10745	<1e-04
Erithacus rubecula : log(Date)	0.810	0.112	1.490	10000	0.020
Model 1 (M0 + TA$_{st}$)					
TA$_{st}$	**0.104**	**0.039**	**0.169**	**10000**	**<0.001**
Model 2 (M0 + TA$_{st}$ × Species)					
Parus major : TA$_{st}$	**0.277**	**0.168**	**0.372**	**1083.200**	**<0.001**
Parus caeruleus : TA$_{st}$	0.079	-0.082	0.237	1000.000	0.364
Acrocephalus scirpaceus : TA$_{st}$	0.040	-0.205	0.275	1000.000	0.744

Sylvia atricapilla : TA $_{st}$	0.021	-0.062	0.113	1000.000	0.642
Sylvia communis : TA $_{st}$	0.044	-0.151	0.261	971.800	0.690
Phylloscopus collybita : TA $_{st}$	0.120	0.001	0.260	843.800	0.066
Aegithalos caudatus : TA $_{st}$	**0.259**	**0.023**	**0.479**	**1156.900**	**0.020**
Turdus merula : TA $_{st}$	-0.107	-0.269	0.067	1000.000	0.188
Erithacus rubecula : TA $_{st}$	**0.121**	**0.011**	**0.224**	**1000.000**	**0.026**
Model 3 (M0 + TA $_{st}$ + TA $_{st}$ × T)					
TA $_{st}$	**0.900**	**0.420**	**1.415**	**10000**	**<0.001**
TA $_{st}$: T_s	**-0.052**	**-0.087**	**-0.022**	**10000**	**<0.001**
Model 4 (M3 + TA × Species)					
Parus major : TA $_{st}$	**1.072**	**0.584**	**1.592**	**10000**	**<0.001**
Parus caeruleus : TA $_{st}$	**0.871**	**0.365**	**1.419**	**10000**	**0.002**
Acrocephalus scirpaceus : TA $_{st}$	**0.819**	**0.297**	**1.398**	**10000**	**0.004**
Sylvia atricapilla : TA $_{st}$	**0.820**	**0.345**	**1.376**	**10000**	**<0.001**
Sylvia communis : TA $_{st}$	**0.886**	**0.295**	**1.432**	**7306**	**0.004**
Phylloscopus collybita : TA $_{st}$	**0.908**	**0.410**	**1.422**	**10000**	**<0.001**
Aegithalos caudatus : TA $_{st}$	**1.045**	**0.489**	**1.588**	**10000**	**<0.001**
Turdus merula : TA $_{st}$	**0.685**	**0.207**	**1.249**	**10000**	**0.010**
Erithacus rubecula : TA $_{st}$	**0.892**	**0.406**	**1.411**	**10000**	**<0.001**
TA $_{st}$: T_s	**-0.052**	**-0.083**	**-0.021**	**10000**	**<0.001**
Model 5 (M4 + TA $_{st}$ × T_s × Species)					
Parus major : TA $_{st}$	**1.411**	**0.133**	**2.705**	**10000**	**0.033**
Parus caeruleus : TA $_{st}$	-0.664	-4.262	2.894	10188	0.711
Acrocephalus scirpaceus : TA $_{st}$	-1.232	-6.204	3.619	10000	0.623
Sylvia atricapilla : TA $_{st}$	**1.848**	**0.895**	**2.792**	**10000**	**<0.001**
Sylvia communis : TA $_{st}$	1.700	-1.779	5.037	9572	0.326
Phylloscopus collybita : TA $_{st}$	0.116	-1.664	1.879	10000	0.904
Aegithalos caudatus : TA $_{st}$	**5.293**	**2.291**	**8.243**	**10000**	**0.002**
Turdus merula : TA $_{st}$	1.627	-0.530	3.634	10000	0.127
Erithacus rubecula : TA $_{st}$	0.179	-0.497	0.867	10000	0.608
Parus major : TA $_{st}$: T_s	**-0.072**	**-0.149**	**-0.000**	**10000**	**0.050**
Parus caeruleus : TA $_{st}$ **: T_s**	0.049	-0.147	0.308	11307	0.686
Acrocephalus scirpaceus : TA $_{st}$ **: T_s**	0.081	-0.233	0.398	12095	0.594
Sylvia atricapilla : TA $_{st}$: T_s	**-0.118**	**-0.177**	**-0.049**	**10000**	**<0.001**
Sylvia communis : TA $_{st}$ **: T_s**	-0.107	-0.303	0.090	11492	0.276
Phylloscopus collybita : TA $_{st}$ **: T_s**	0.001	-0.114	0.126	10000	0.950
Aegithalos caudatus : TA $_{st}$: T_s	**-0.324**	**-0.493**	**-0.129**	**8730**	**<0.001**
Turdus merula : TA $_{st}$ **: T_s**	-0.112	-0.236	0.031	11021	0.098
Erithacus rubecula : TA $_{st}$ **: T_s**	-0.002	-0.045	0.043	10000	0.924

Random effects	Variance	Lower 95% CI	Upper 95% CI	Effective sampling
Observer	0.179	0.055	0.313	5709
Site (residual)	0.435	0.329	0.543	10000
Year (residual)	0.0102	0.002	0.022	10000

Residual	4.827	4.753	4.895	10000

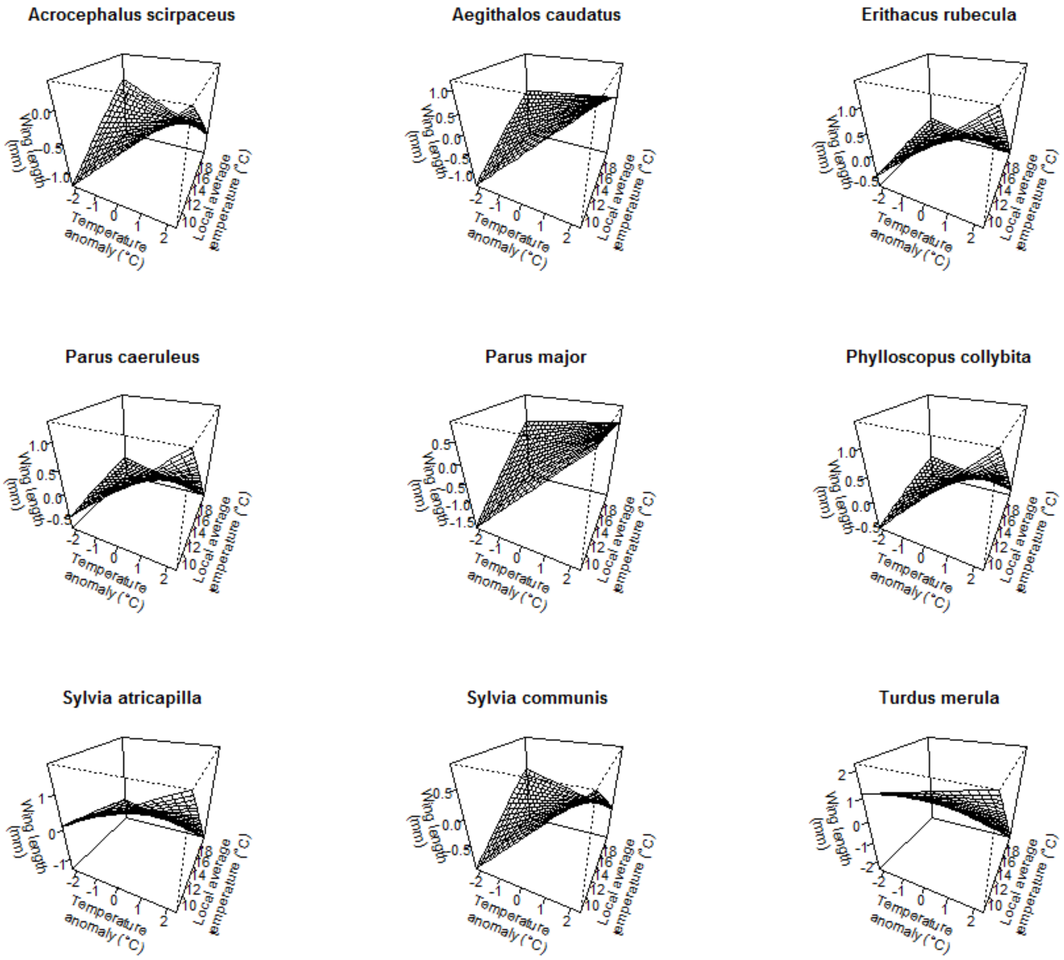

Fig. S3a Species-specific response of juvenile wing length to temperature anomaly along gradients in local average temperature for nine songbird species from France. Predicted values were obtained from MCMCglmm assuming a differential response of temperature anomaly between species, and an overall decrease of this response with local average temperature (Model 4). Local average temperature is the mean breeding period temperature of a given site for the period 2000-2014.

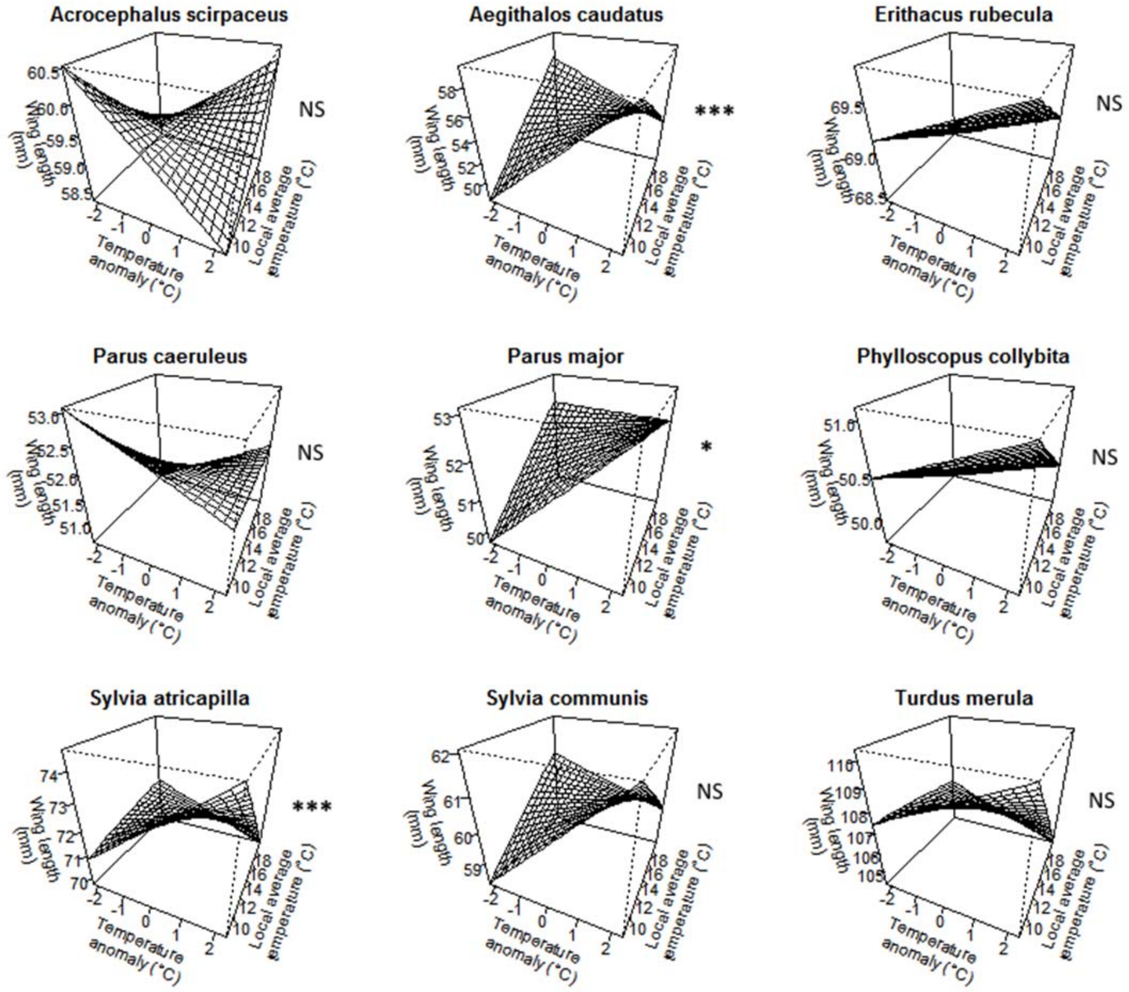

Fig. S3b Species-specific response of juvenile wing length to temperature anomaly along gradients in local average temperature for nine songbird species from France. Predicted values were obtained from MCMCglmm assuming a differential response of temperature anomaly between species, and a differential decrease of this response with local average temperature (Model 5). Local average temperature is the mean breeding period temperature of a given site for the period 2000-2014. The interactive effect was significant for three species (*, pMCMC <0.05; ***, pMCMC < 0.001; NS, non-significant).

Fig S4a. Trace plots of the models 4. ano.t is the temperature anomaly effect; sitem.t is the local average temperature effect; log(juldate) is the log-transformed effect of Julian date.

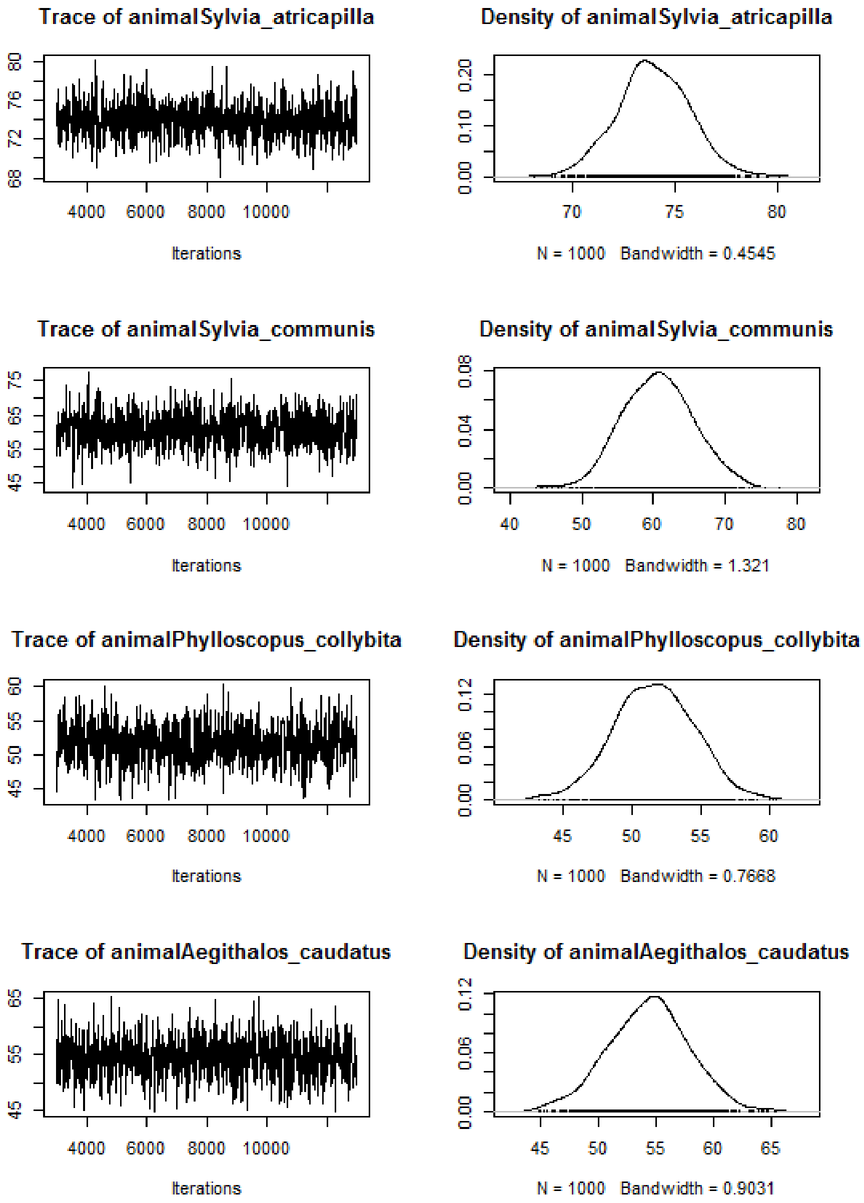

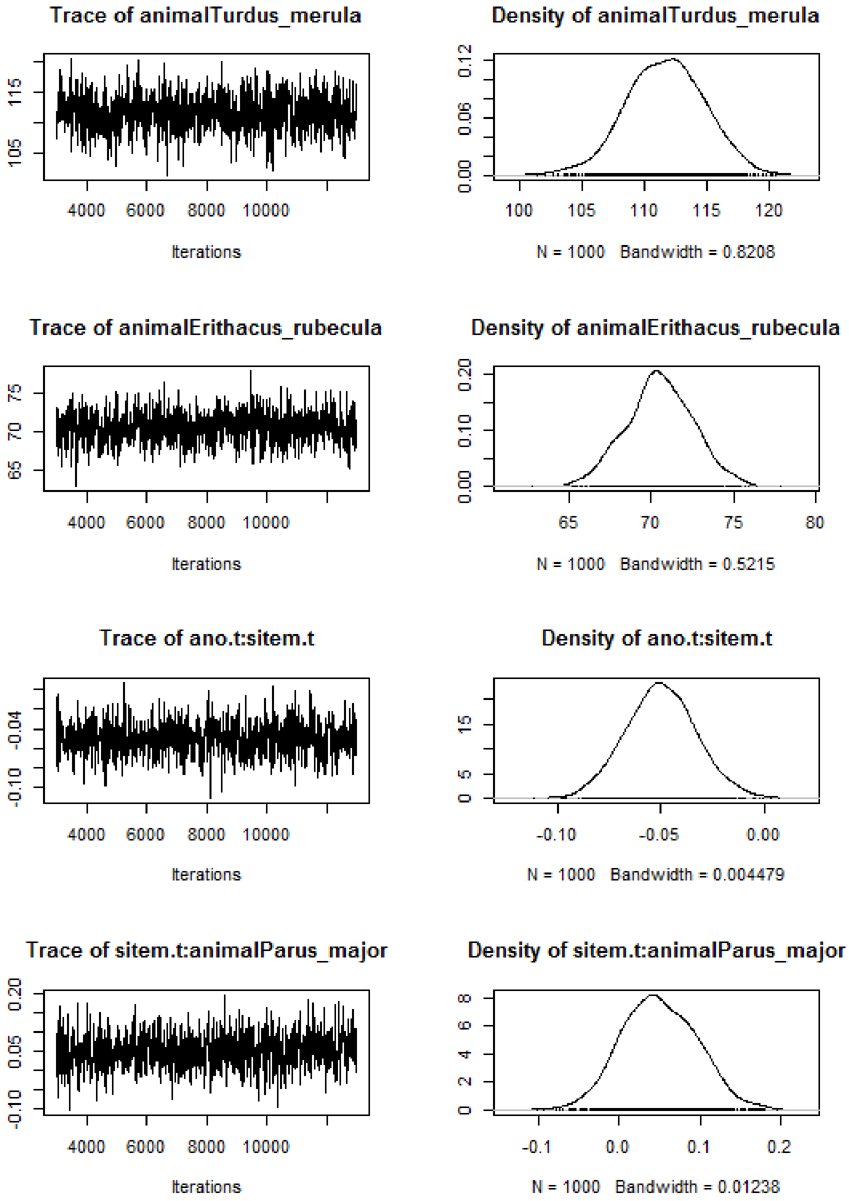
Trace of animalTurdus_merula
105
115
4000
6000
8000
10000
Iterations
Density of animalTurdus_merula
0.00
0.06
0.12
100
105
110
115
120
N = 1000 Bandwidth = 0.8208
Trace of animalErithacus_rubecula
65
70
75
4000
6000
8000
10000
Iterations
Density of animalErithacus_rubecula
0.00
0.10
0.20
65
70
75
80
N = 1000 Bandwidth = 0.5215
Trace of ano.t:sitem.t
-0.10
-0.04
4000
6000
8000
10000
Iterations
Density of ano.t:sitem.t
0
5
15
-0.10
-0.05
0.00
N = 1000 Bandwidth = 0.004479
Trace of sitem.t:animalParus_major
-0.10
0.05
0.20
4000
6000
8000
10000
Iterations
Density of sitem.t:animalParus_major
0
2
4
6
8
-0.1
0.0
0.1
0.2
N = 1000 Bandwidth = 0.01238

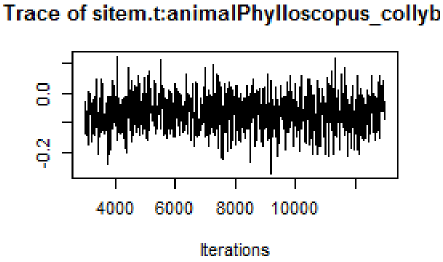
Trace of sitem.t:animalPhylloscopus_collyb
0.0
-0.2
4000
6000
8000
10000
Iterations

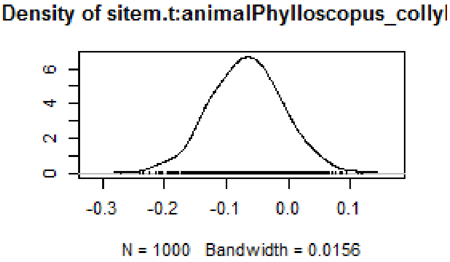
Density of sitem.t:animalPhylloscopus_collyl
6
4
2
0
-0.3
-0.2
-0.1
0.0
0.1
N = 1000 Bandwidth = 0.0156

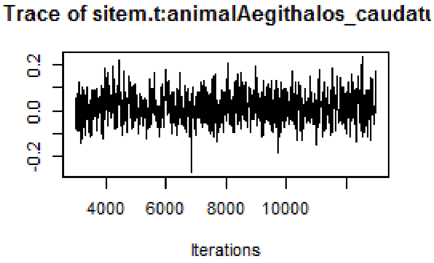
Trace of sitem.t:animalAegithalos_caudatu
0.2
0.0
-0.2
4000
6000
8000
10000
Iterations

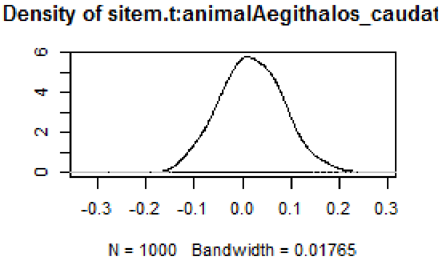
Density of sitem.t:animalAegithalos_caudat
6
4
2
0
-0.3
-0.2
-0.1
0.0
0.1
0.2
0.3
N = 1000 Bandwidth = 0.01765

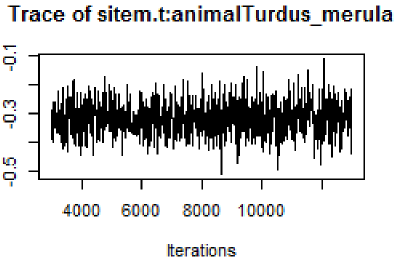
Trace of sitem.t:animalTurdus_merula
-0.1
-0.3
-0.5
4000
6000
8000
10000
Iterations

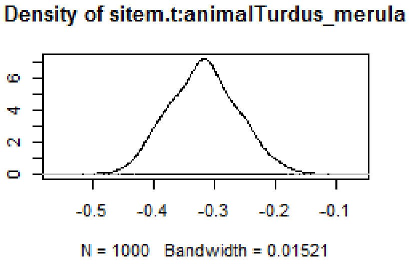
Density of sitem.t:animalTurdus_merula
6
4
2
0
-0.5
-0.4
-0.3
-0.2
-0.1
N = 1000 Bandwidth = 0.01521

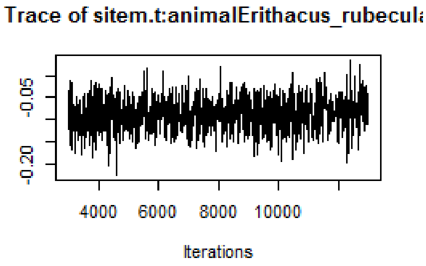
Trace of sitem.t:animalErithacus_rubecula
-0.05
-0.20
4000
6000
8000
10000
Iterations

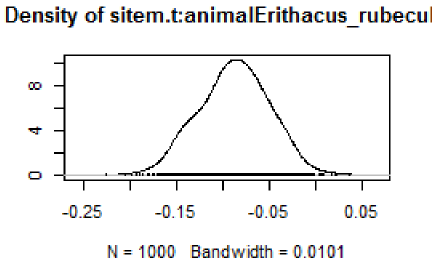
Density of sitem.t:animalErithacus_rubecul
8
4
0
-0.25
-0.15
-0.05
0.05
N = 1000 Bandwidth = 0.0101

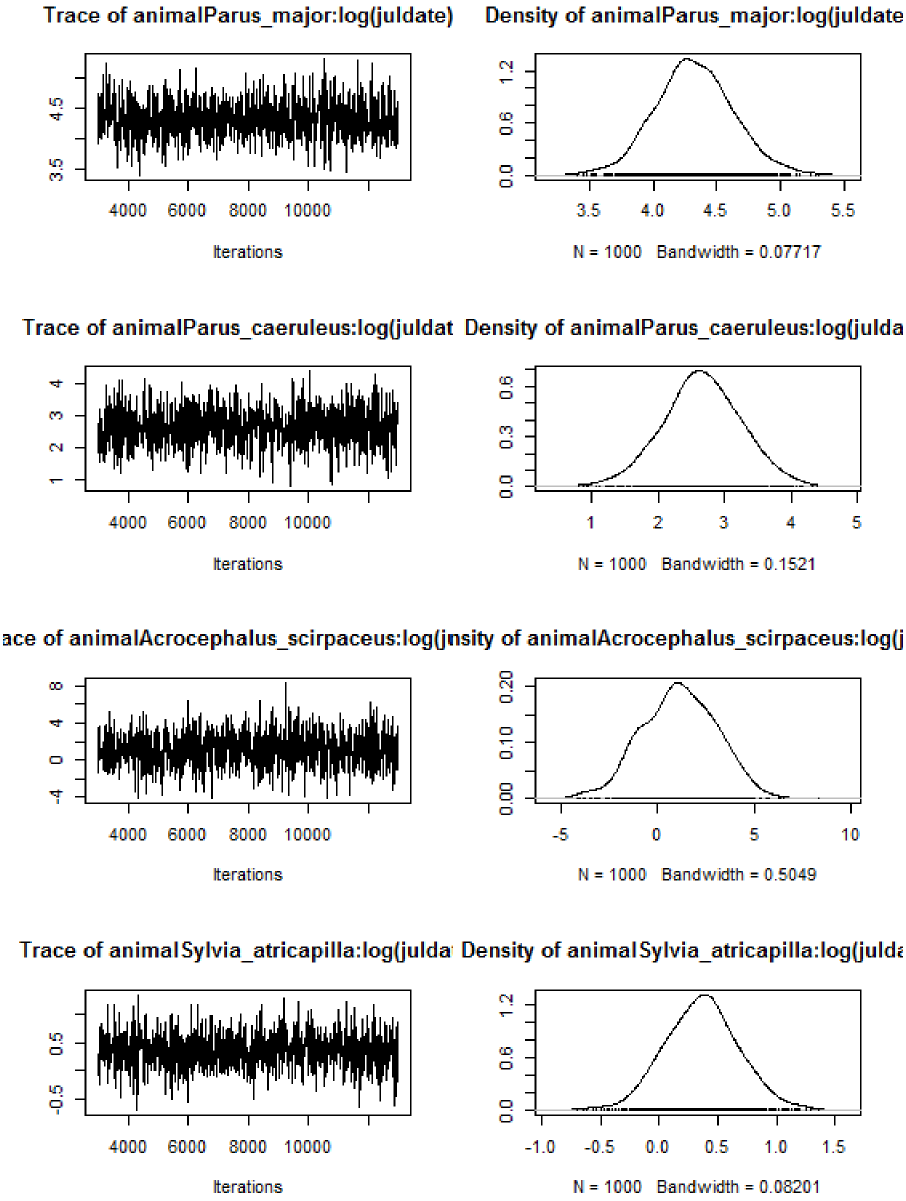
Trace of animalParus_major:log(juldate)
Density of animalParus_major:log(juldate
3.5
4.5
4000
6000
8000
10000
Iterations
0.0
0.6
1.2
3.5
4.0
4.5
5.0
5.5
N = 1000 Bandwidth = 0.07717
Trace of animalParus_caeruleus:log(juldat
Density of animalParus_caeruleus:log(julda
1
2
3
4
4000
6000
8000
10000
Iterations
0.0
0.3
0.6
1
2
3
4
5
N = 1000 Bandwidth = 0.1521
ace of animalAcrocephalus_scirpaceus:log(j
nsity of animalAcrocephalus_scirpaceus:log(j
-4
0
4
8
4000
6000
8000
10000
Iterations
0.00
0.10
0.20
-5
0
5
10
N = 1000 Bandwidth = 0.5049
Trace of animalSylvia_atricapilla:log(julda
Density of animalSylvia_atricapilla:log(julda
-0.5
0.5
4000
6000
8000
10000
Iterations
0.0
0.6
1.2
-1.0
-0.5
0.0
0.5
1.0
1.5
N = 1000 Bandwidth = 0.08201

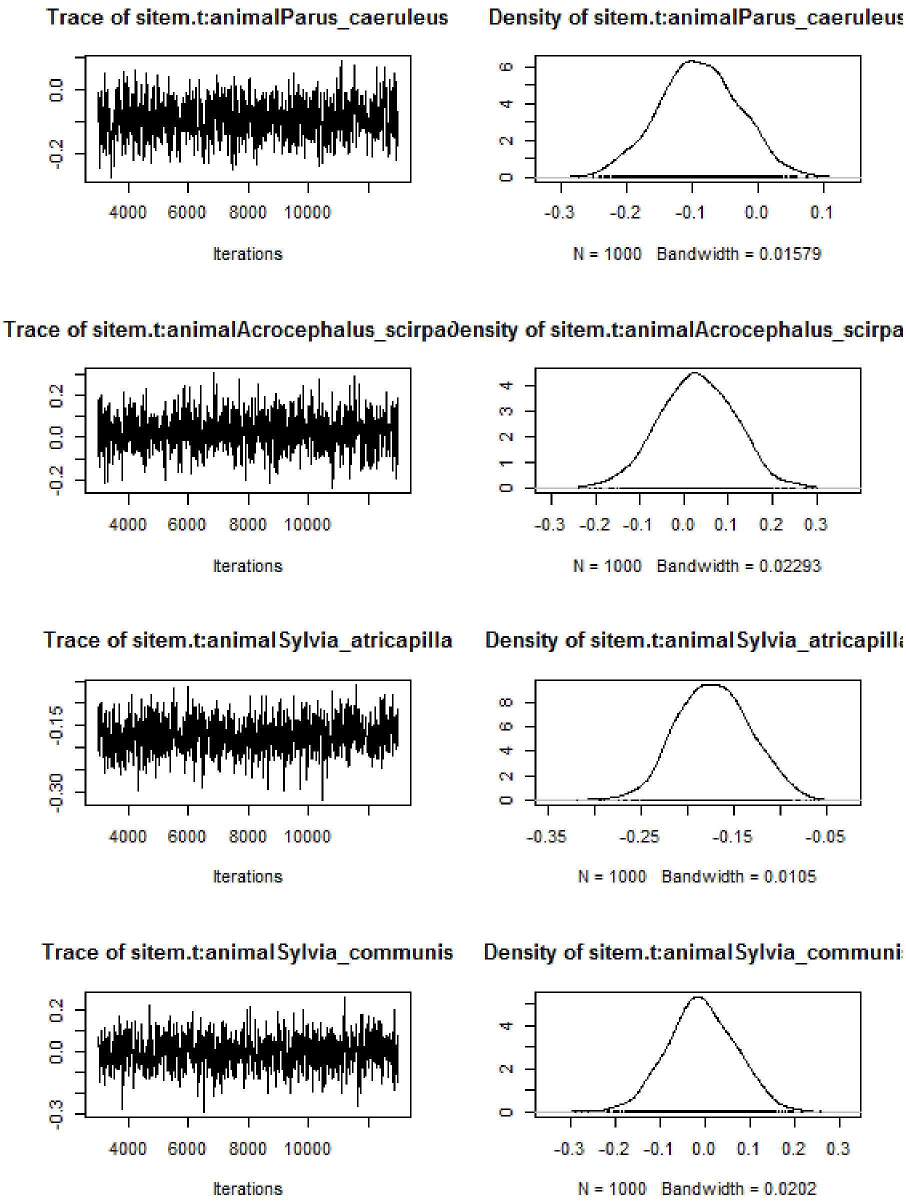
Trace of sitem.t:animalParus_caeruleus
0.0
-0.2
4000
6000
8000
10000
Iterations
Density of sitem.t:animalParus_caeruleu
6
4
2
0
-0.3
-0.2
-0.1
0.0
0.1
N = 1000 Bandwidth = 0.01579
Trace of sitem.t:animalAcrocephalus_scirpa
0.2
0.0
-0.2
4000
6000
8000
10000
Iterations
ensity of sitem.t:animalAcrocephalus_scirpa
4
3
2
1
0
-0.3
-0.2
-0.1
0.0
0.1
0.2
0.3
N = 1000 Bandwidth = 0.02293
Trace of sitem.t:animalSylvia_atricapilla
-0.15
-0.30
4000
6000
8000
10000
Iterations
Density of sitem.t:animalSylvia_atricapill
8
6
4
2
0
-0.35
-0.25
-0.15
-0.05
N = 1000 Bandwidth = 0.0105
Trace of sitem.t:animalSylvia_communis
0.2
0.0
-0.3
4000
6000
8000
10000
Iterations
Density of sitem.t:animalSylvia_communi
4
2
0
-0.3
-0.2
-0.1
0.0
0.1
0.2
0.3
N = 1000 Bandwidth = 0.0202

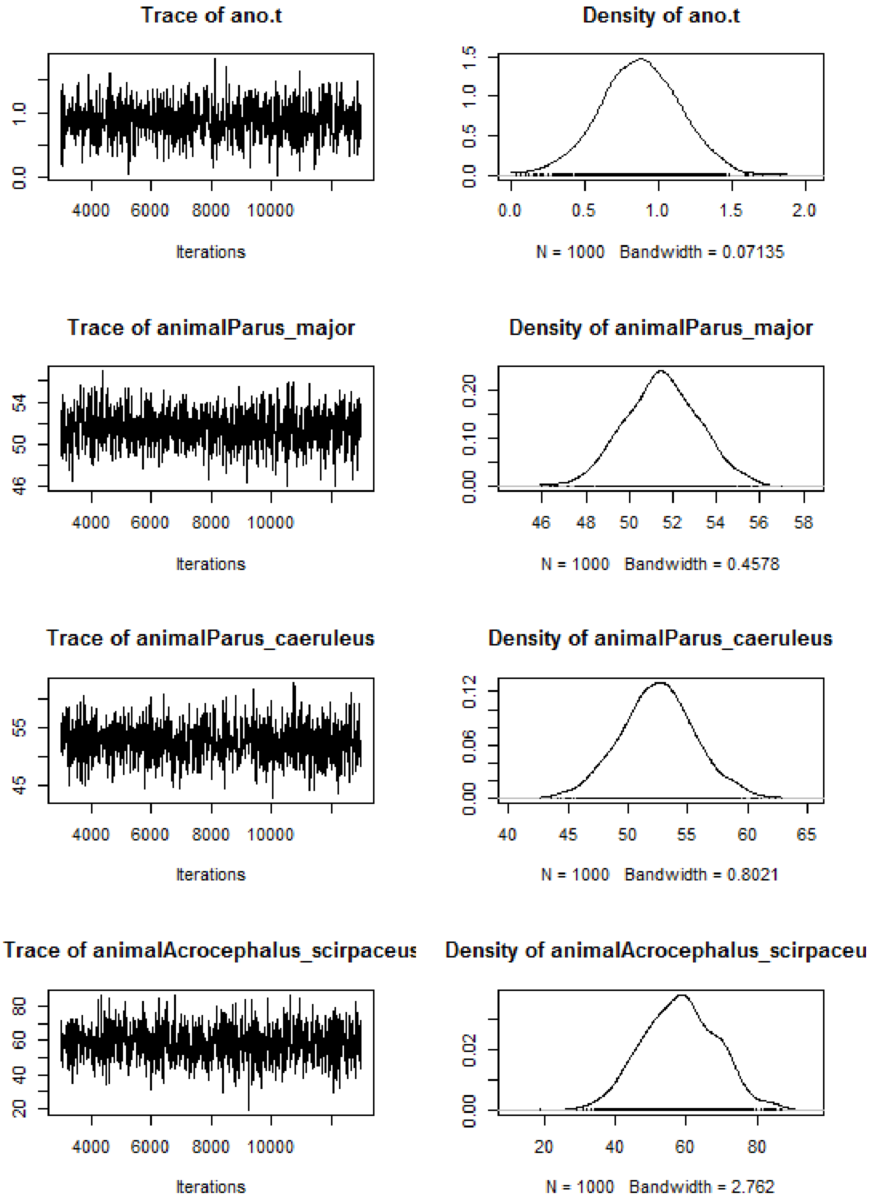
Trace of ano.t

Density of ano.t

Trace of animalParus_major

Density of animalParus_major

Trace of animalParus_caeruleus

Density of animalParus_caeruleus

Trace of animalAcrocephalus_scirpaceus

Density of animalAcrocephalus_scirpaceu

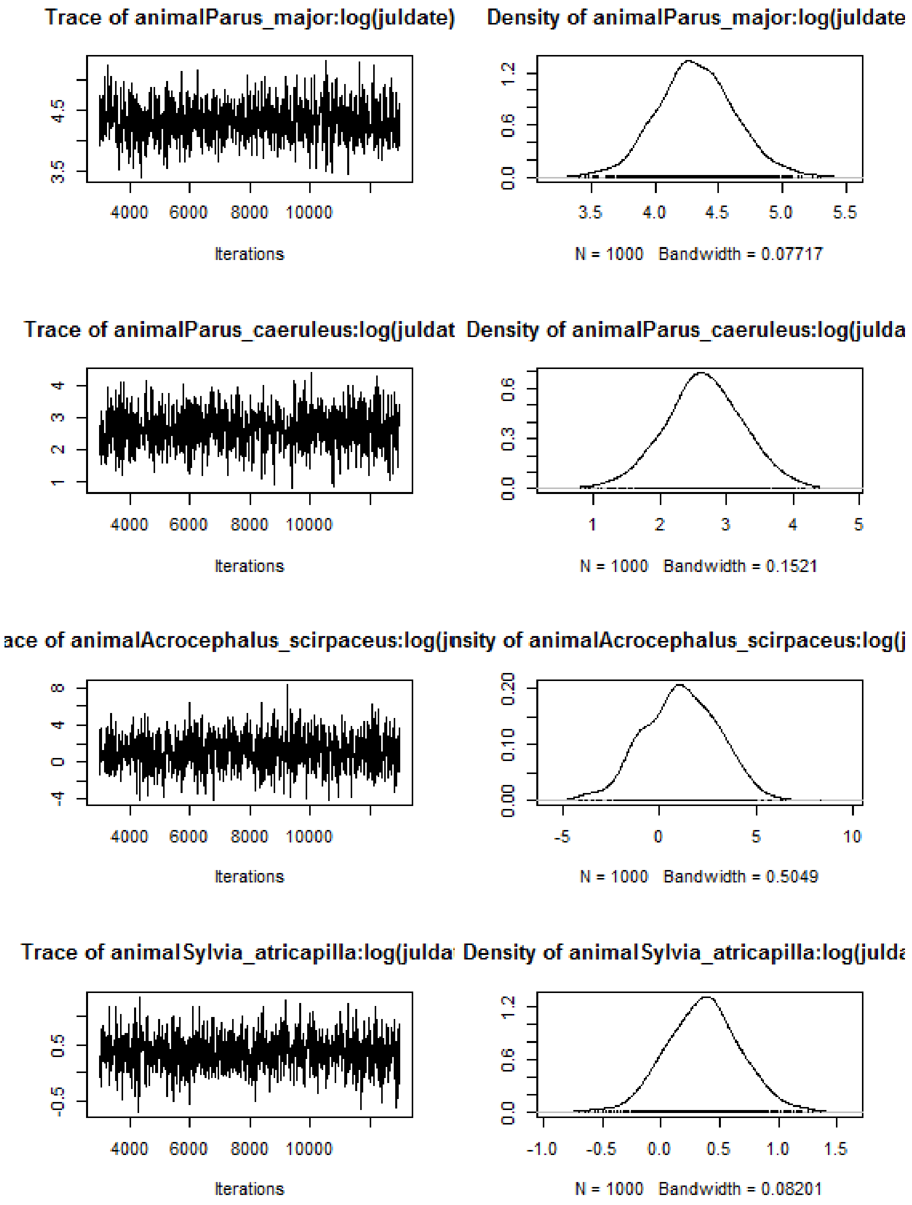
Trace of animalParus_major:log(juldate)
Density of animalParus_major:log(juldate
3.5
4.5
4000
6000
8000
10000
Iterations
0.0
0.6
1.2
3.5
4.0
4.5
5.0
5.5
N = 1000 Bandwidth = 0.07717
Trace of animalParus_caeruleus:log(juldat
Density of animalParus_caeruleus:log(julda
1
2
3
4
Iterations
0.0
0.3
0.6
5
N = 1000 Bandwidth = 0.1521
ace of animalAcrocephalus_scirpaceus:log(j
nsity of animalAcrocephalus_scirpaceus:log(j
-4
0
8
0.00
0.10
0.20
-5
10
N = 1000 Bandwidth = 0.5049
Trace of animalSylvia_atricapilla:log(julda
Density of animalSylvia_atricapilla:log(julda
-0.5
0.5
-1.0
1.0
1.5
N = 1000 Bandwidth = 0.08201

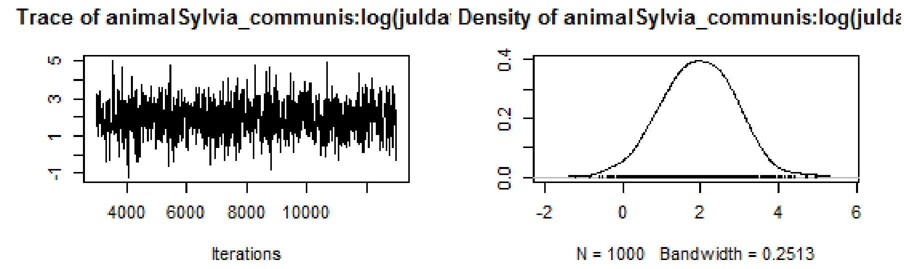
Trace of animalSylvia_communis:log(julda
Density of animalSylvia_communis:log(julda
-1
1
3
5
4000
6000
8000
10000
Iterations
0.0
0.2
0.4
-2
0
2
4
6
N = 1000 Bandwidth = 0.2513

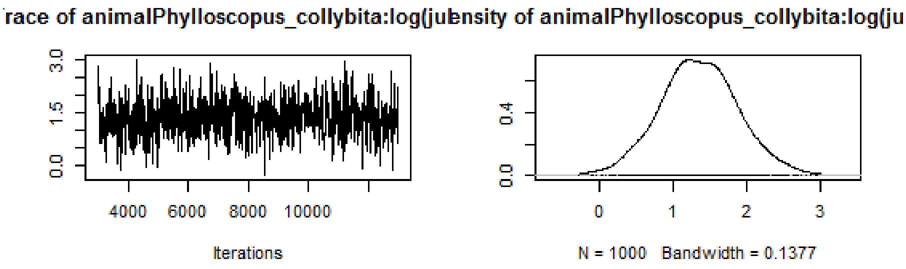
race of animalPhylloscopus_collybita:log(ju
ensity of animalPhylloscopus_collybita:log(ju
0.0
1.5
3.0
4000
6000
8000
10000
Iterations
0.0
0.4
0
1
2
3
N = 1000 Bandwidth = 0.1377

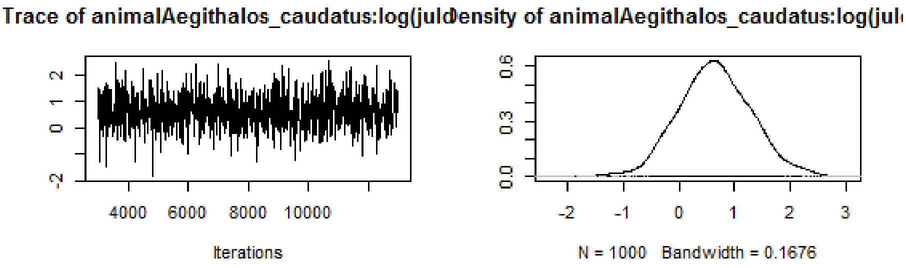
Trace of animalAegithalos_caudatus:log(juld
ensity of animalAegithalos_caudatus:log(jul
-2
0
1
2
4000
6000
8000
10000
Iterations
0.0
0.3
0.6
-2
-1
0
1
2
3
N = 1000 Bandwidth = 0.1676

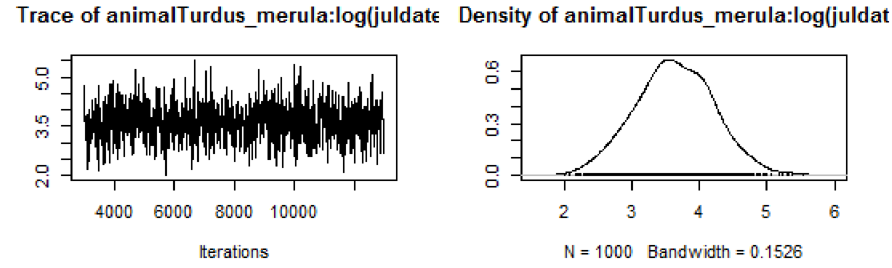
Trace of animalTurdus_merula:log(juldate
Density of animalTurdus_merula:log(juldat
2.0
3.5
5.0
4000
6000
8000
10000
Iterations
0.0
0.3
0.6
2
3
4
5
6
N = 1000 Bandwidth = 0.1526

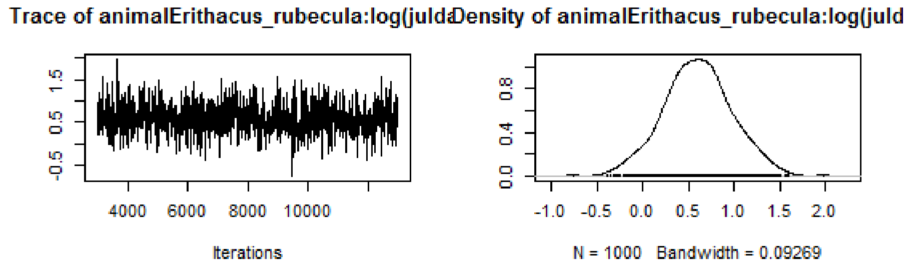
Trace of animalErithacus_rubecula:log(julda
Density of animalErithacus_rubecula:log(juld
-0.5
0.5
1.5
4000
6000
8000
10000
Iterations
0.0
0.4
0.8
-1.0
-0.5
0.0
0.5
1.0
1.5
2.0
N = 1000 Bandwidth = 0.09269

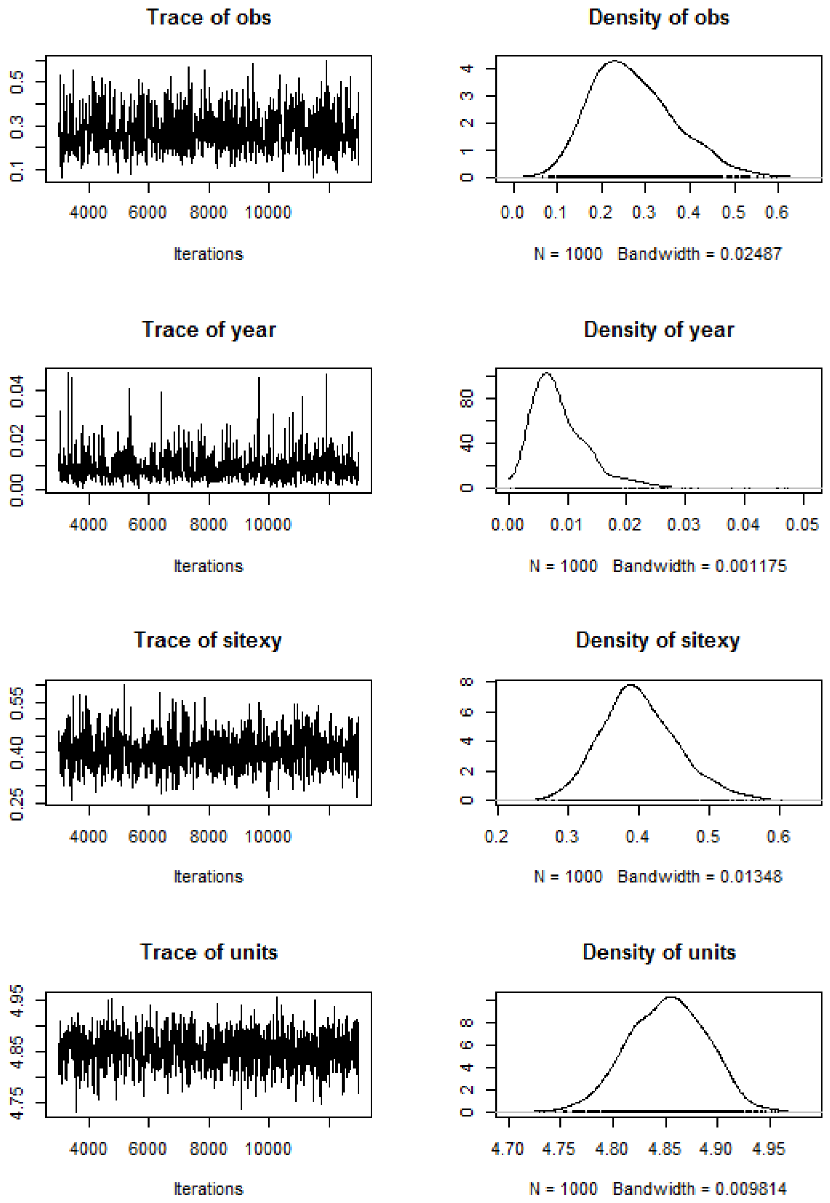
Trace of obs
0.1
0.3
0.5
4000
6000
8000
10000
Iterations
Density of obs
0
1
2
3
4
0.0
0.1
0.2
0.3
0.4
0.5
0.6
N = 1000 Bandwidth = 0.02487
Trace of year
0.00
0.02
0.04
4000
6000
8000
10000
Iterations
Density of year
0
40
80
0.00
0.01
0.02
0.03
0.04
0.05
N = 1000 Bandwidth = 0.001175
Trace of sitexy
0.25
0.40
0.55
4000
6000
8000
10000
Iterations
Density of sitexy
0
2
4
6
8
0.2
0.3
0.4
0.5
0.6
N = 1000 Bandwidth = 0.01348
Trace of units
4.75
4.85
4.95
4000
6000
8000
10000
Iterations
Density of units
0
2
4
6
8
4.70
4.75
4.80
4.85
4.90
4.95
N = 1000 Bandwidth = 0.009814

Fig S4b Trace plots of the models 5. ano.t is the temperature anomaly effect; sitem.t is the local average temperature effect; log(juldate) is the log-transformed effect of Julian date.

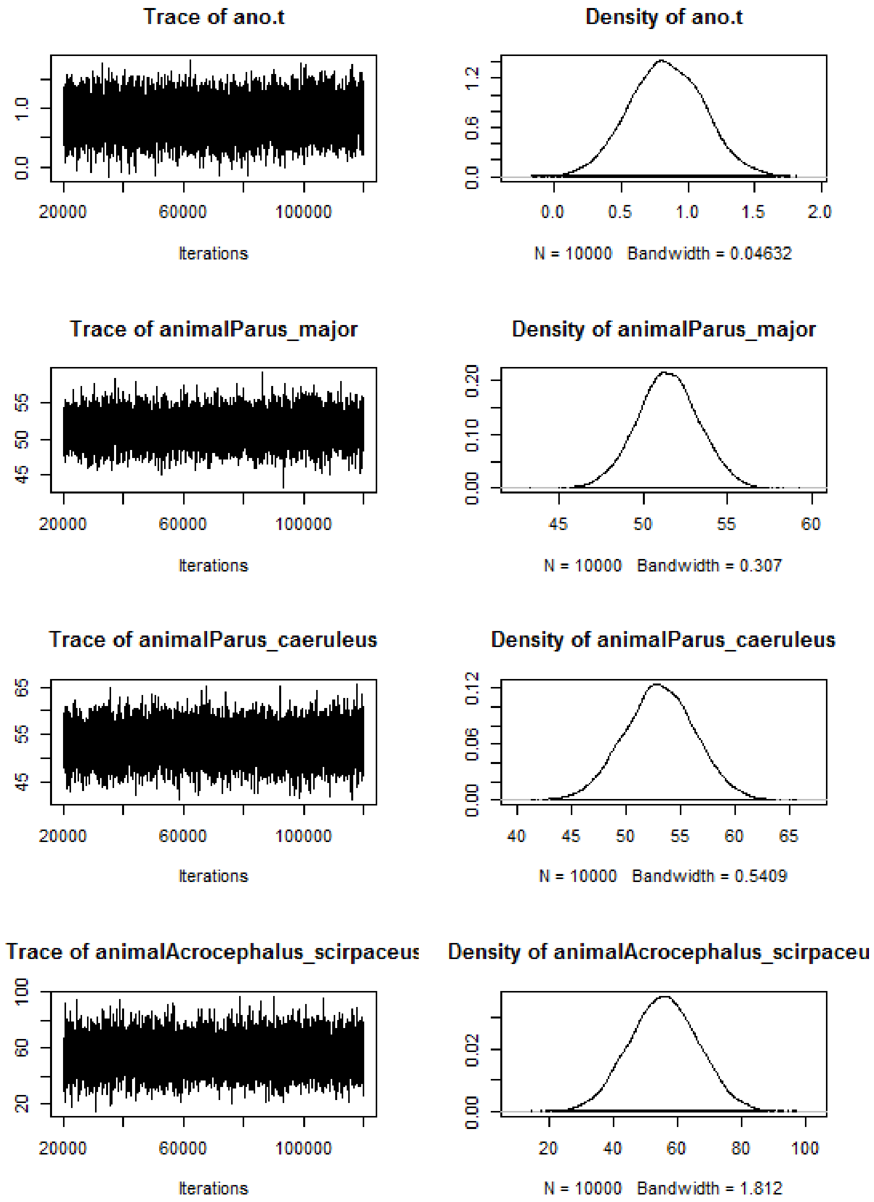

Trace of animalSylvia_atricapilla

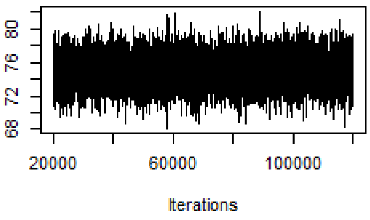

Density of animalSylvia_atricapilla

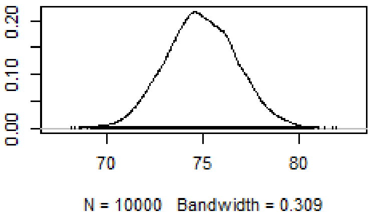

Trace of animalSylvia_communis

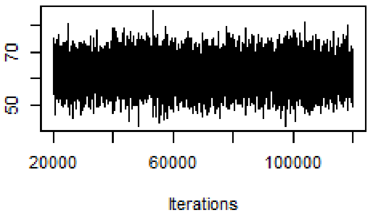

Density of animalSylvia_communis

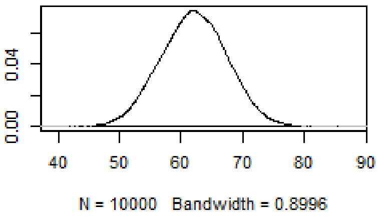

Trace of animalPhylloscopus_collybita

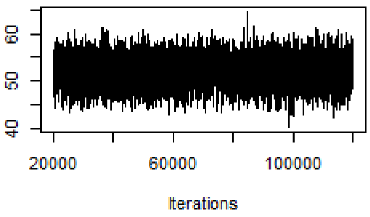

Density of animalPhylloscopus_collybita

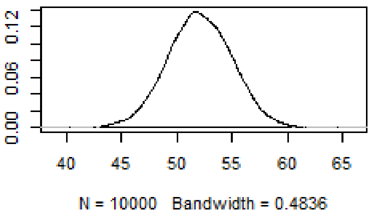

Trace of animalAegithalos_caudatus

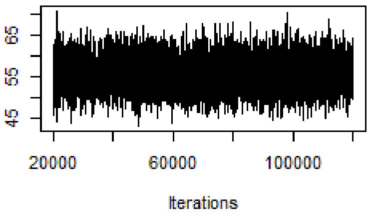

Density of animalAegithalos_caudatus

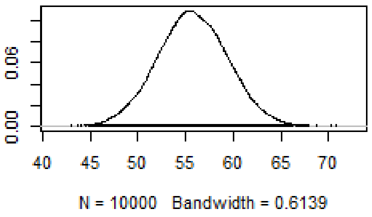

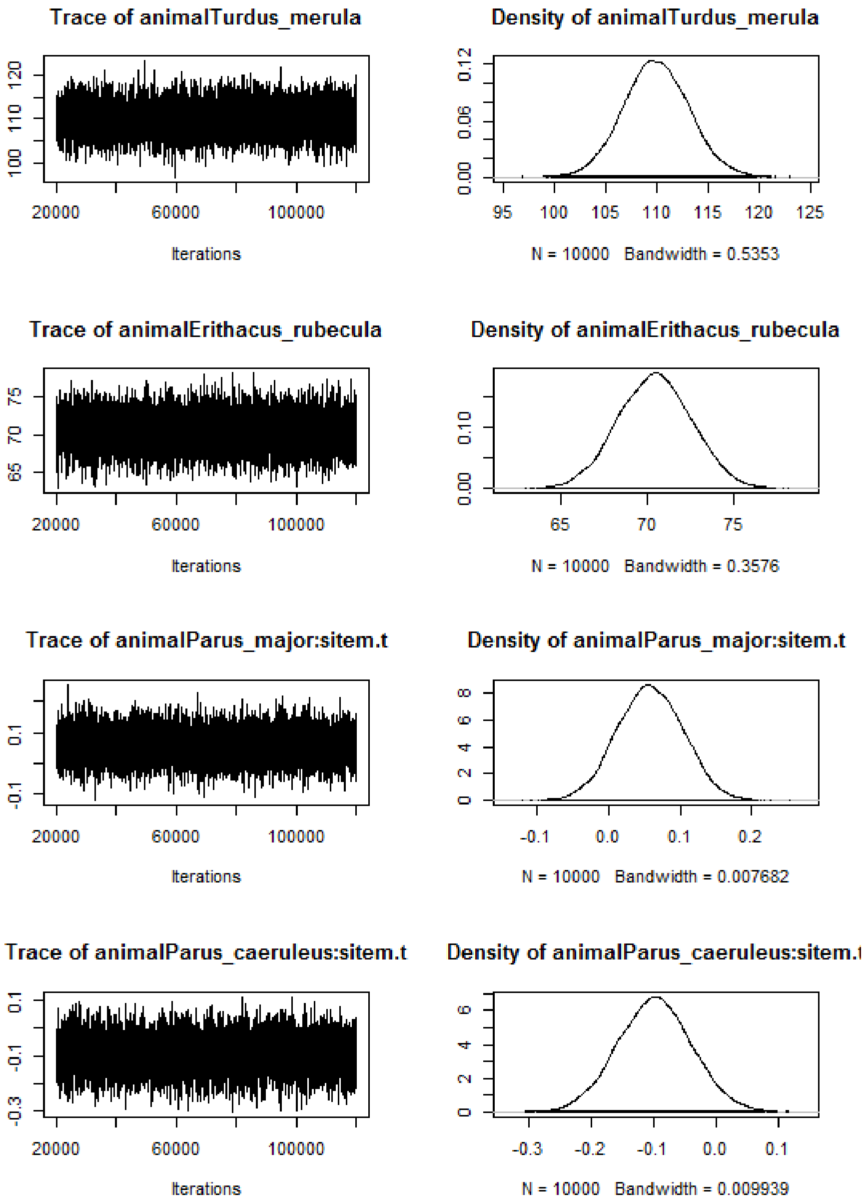
Trace of animalTurdus_merula
100
110
120
20000
60000
100000
Iterations
Density of animalTurdus_merula
0.00
0.06
0.12
95
100
105
110
115
120
125
N = 10000   Bandwidth = 0.5353
Trace of animalErithacus_rubecula
65
70
75
20000
60000
100000
Iterations
Density of animalErithacus_rubecula
0.00
0.10
65
70
75
N = 10000   Bandwidth = 0.3576
Trace of animalParus_major:sitem.t
-0.1
0.1
20000
60000
100000
Iterations
Density of animalParus_major:sitem.t
0
2
4
6
8
-0.1
0.0
0.1
0.2
N = 10000   Bandwidth = 0.007682
Trace of animalParus_caeruleus:sitem.t
-0.3
-0.1
0.1
20000
60000
100000
Iterations
Density of animalParus_caeruleus:sitem.t
0
2
4
6
-0.3
-0.2
-0.1
0.0
0.1
N = 10000   Bandwidth = 0.009939

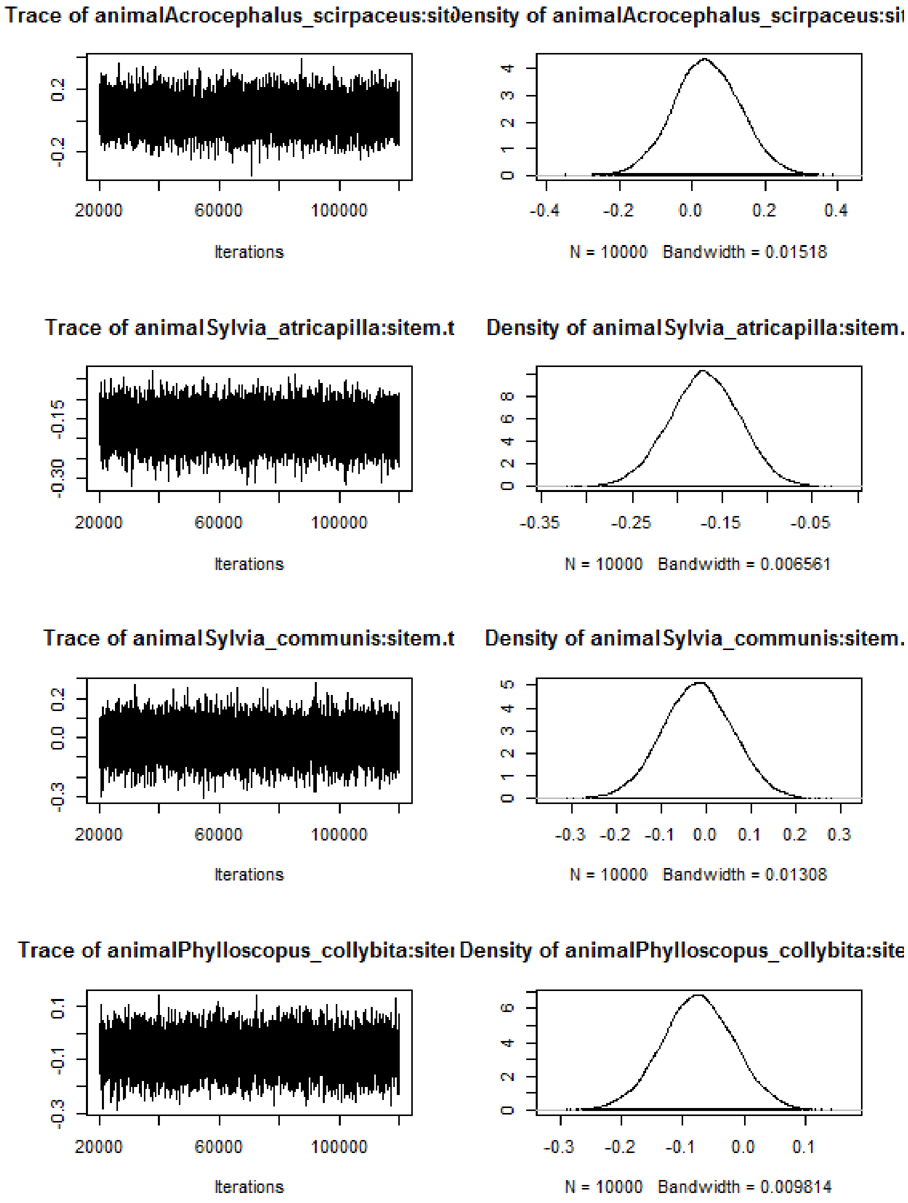

Trace of animalAcrocephalus_scirpaceus:sit
Density of animalAcrocephalus_scirpaceus:si
0.2
-0.2
20000
60000
100000
Iterations
0 1 2 3 4
-0.4 -0.2 0.0 0.2 0.4
N = 10000 Bandwidth = 0.01518
Trace of animalSylvia_atricapilla:sitem.t
Density of animalSylvia_atricapilla:sitem.
-0.15
-0.30
20000
60000
100000
Iterations
0 2 4 6 8
-0.35 -0.25 -0.15 -0.05
N = 10000 Bandwidth = 0.006561
Trace of animalSylvia_communis:sitem.t
Density of animalSylvia_communis:sitem.
0.2
0.0
-0.3
20000
60000
100000
Iterations
0 1 2 3 4 5
-0.3 -0.2 -0.1 0.0 0.1 0.2 0.3
N = 10000 Bandwidth = 0.01308
Trace of animalPhylloscopus_collybita:site
Density of animalPhylloscopus_collybita:site
0.1
-0.1
-0.3
20000
60000
100000
Iterations
0 2 4 6
-0.3 -0.2 -0.1 0.0 0.1
N = 10000 Bandwidth = 0.009814

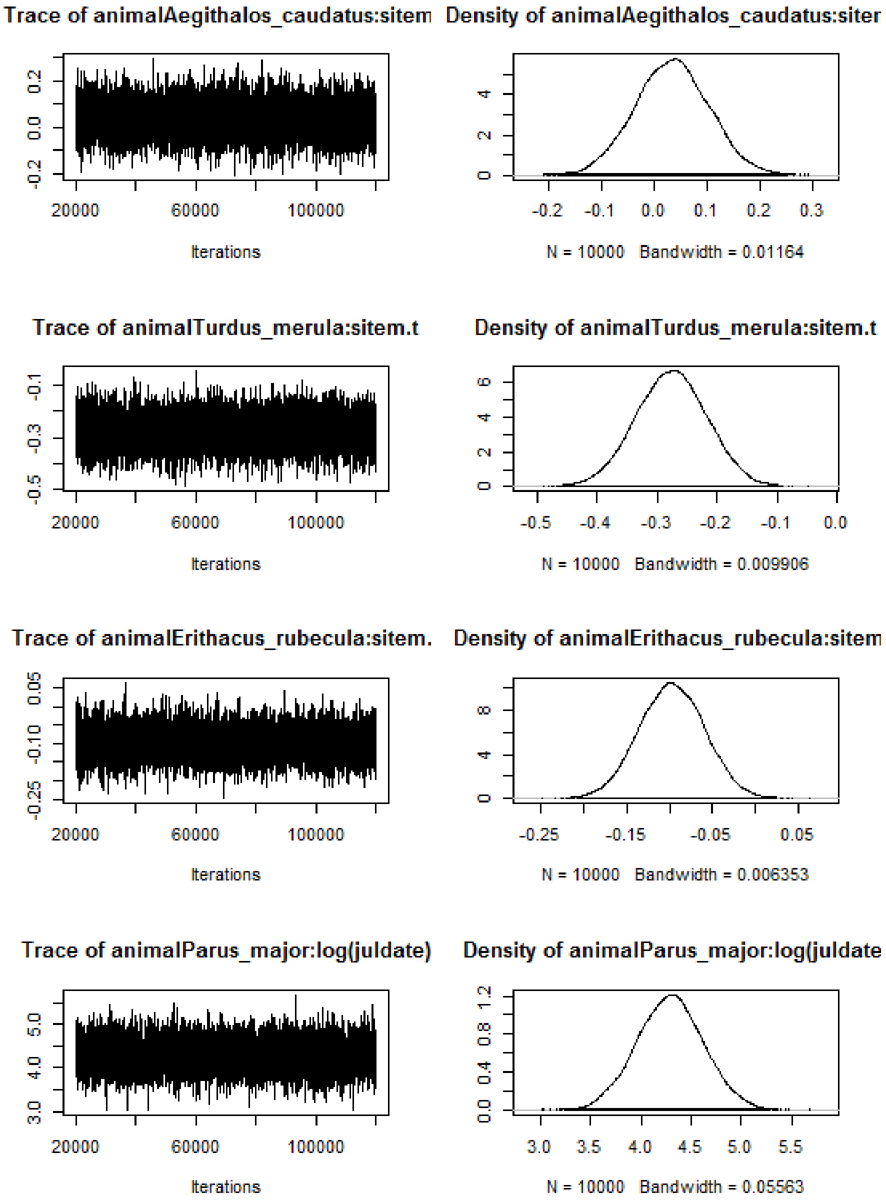
Trace of animalAegithalos_caudatus:sitem
0.2
0.0
-0.2
20000
60000
100000
Iterations
Density of animalAegithalos_caudatus:siter
4
2
0
-0.2
-0.1
0.0
0.1
0.2
0.3
N = 10000 Bandwidth = 0.01164
Trace of animalTurdus_merula:sitem.t
-0.1
-0.3
-0.5
20000
60000
100000
Iterations
Density of animalTurdus_merula:sitem.t
6
4
2
0
-0.5
-0.4
-0.3
-0.2
-0.1
0.0
N = 10000 Bandwidth = 0.009906
Trace of animalErithacus_rubecula:sitem.
0.05
-0.10
-0.25
20000
60000
100000
Iterations
Density of animalErithacus_rubecula:sitem
8
4
0
-0.25
-0.15
-0.05
0.05
N = 10000 Bandwidth = 0.006353
Trace of animalParus_major:log(juldate)
5.0
4.0
3.0
20000
60000
100000
Iterations
Density of animalParus_major:log(juldate
1.2
0.8
0.4
0.0
3.0
3.5
4.0
4.5
5.0
5.5
N = 10000 Bandwidth = 0.05563

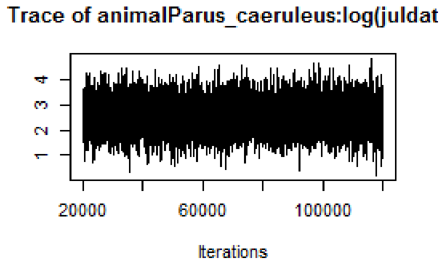

Trace of animalParus_caeruleus:log(juldat

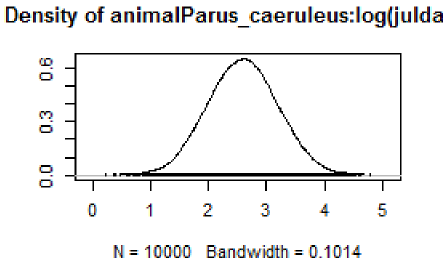

Density of animalParus_caeruleus:log(julda

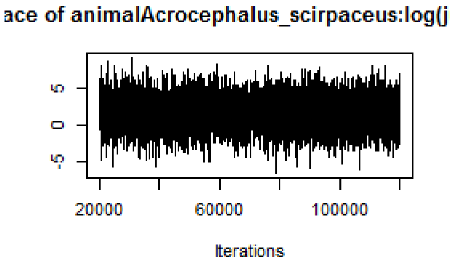

ace of animalAcrocephalus_scirpaceus:log(j

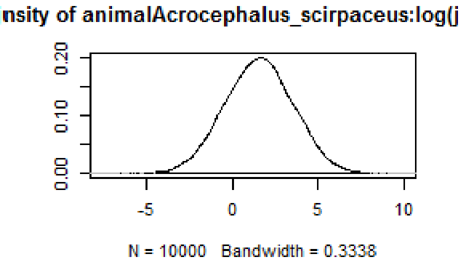

nsity of animalAcrocephalus_scirpaceus:log(j

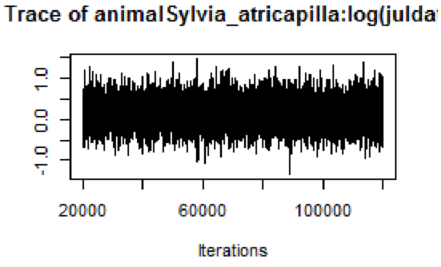

Trace of animalSylvia_atricapilla:log(julda

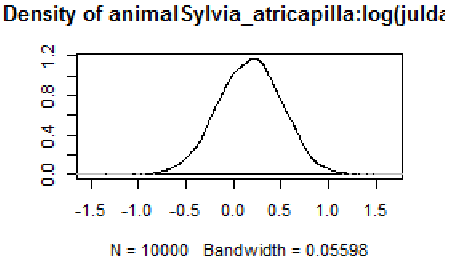

Density of animalSylvia_atricapilla:log(julda

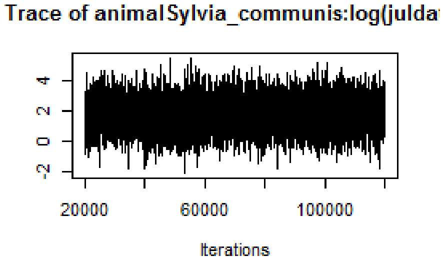

Trace of animalSylvia_communis:log(julda

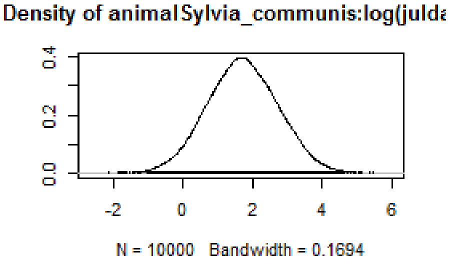

Density of animalSylvia_communis:log(julda race of animalPhylloscopus_collybita:log(jul

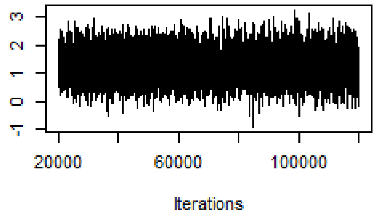

ensity of animalPhylloscopus_collybita:log(ju

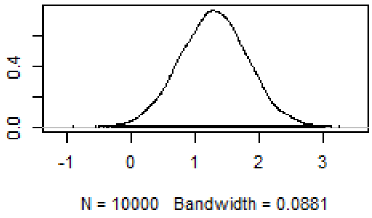

Trace of animalAegithalos_caudatus:log(juld

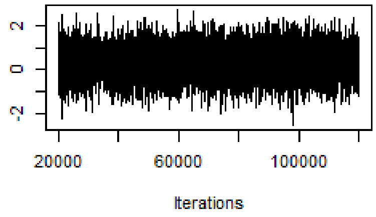

ensity of animalAegithalos_caudatus:log(jul

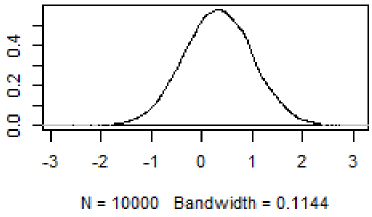

Trace of animalTurdus_merula:log(juldate

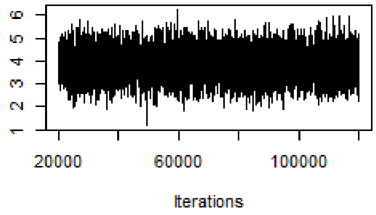

Density of animalTurdus_merula:log(juldat

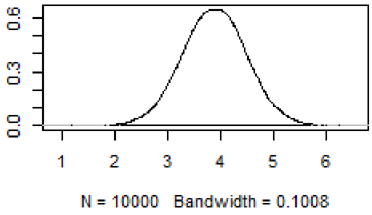

Trace of animalErithacus_rubecula:log(julda

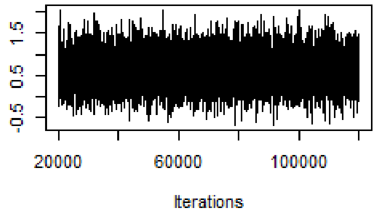

Density of animalErithacus_rubecula:log(juld

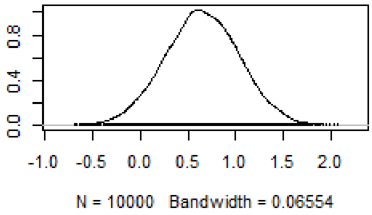

Trace of ano.t:animalParus_major:sitem.

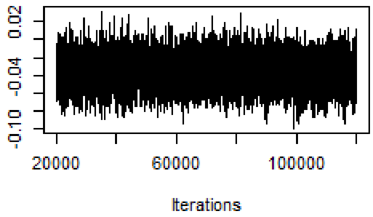

Density of ano.t:animalParus_major:sitem

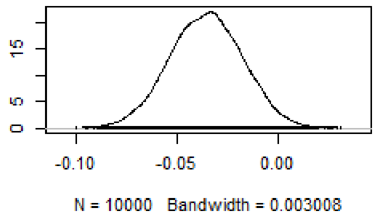

Trace of ano.t:animalParus_caeruleus:siter

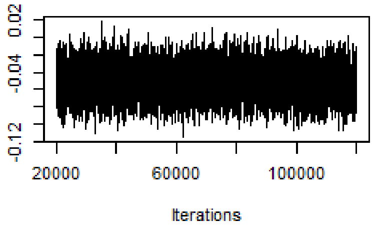

Density of ano.t:animalParus_caeruleus:site

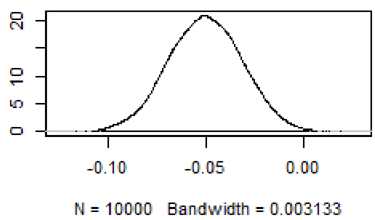

ıce of ano.t:animalAcrocephalus_scirpaceus

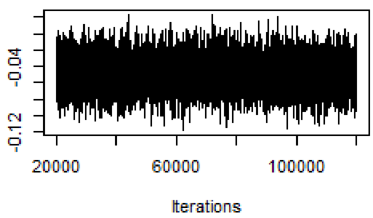

ısity of ano.t:animalAcrocephalus_scirpaceus

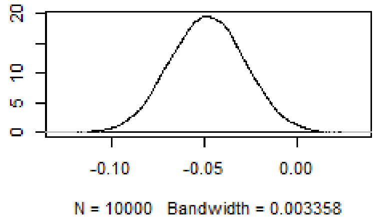

Trace of ano.t:animalSylvia_atricapilla:site

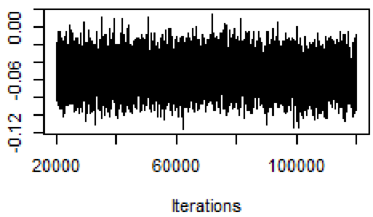

Density of ano.t:animalSylvia_atricapilla:site

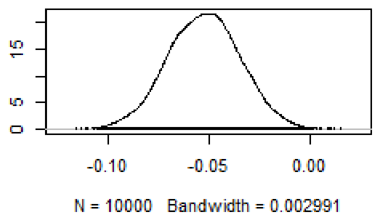

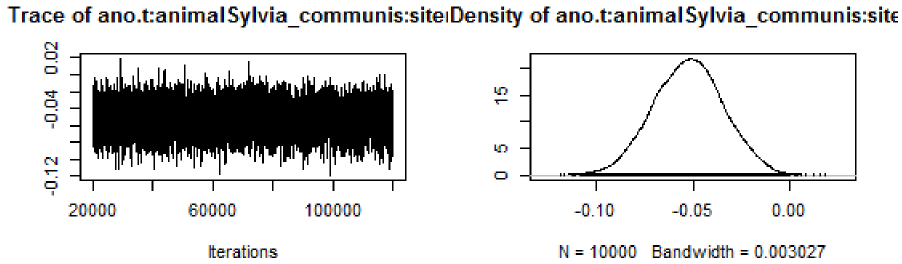
Trace of ano.t:animalSylvia_communis:site
Density of ano.t:animalSylvia_communis:site
0.02
-0.04
-0.12
20000
60000
100000
Iterations
0
5
15
-0.10
-0.05
0.00
N = 10000 Bandwidth = 0.003027

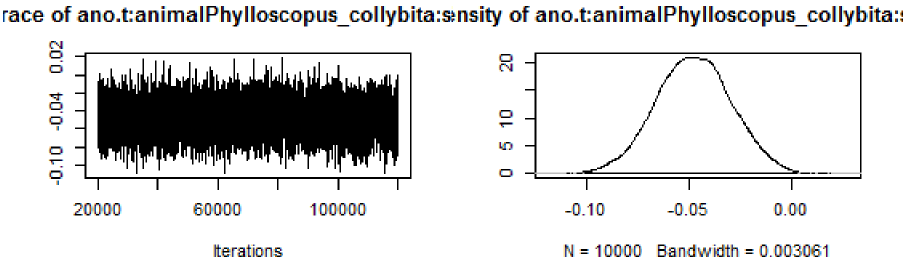
race of ano.t:animalPhylloscopus_collybita:s
nsity of ano.t:animalPhylloscopus_collybita:
0.02
-0.04
-0.10
20000
60000
100000
Iterations
0
5
10
20
-0.10
-0.05
0.00
N = 10000 Bandwidth = 0.003061

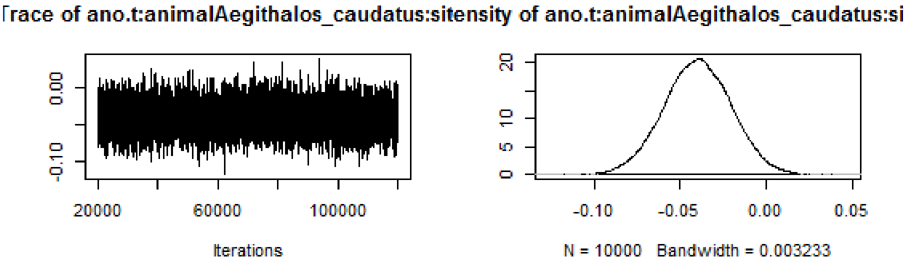
Trace of ano.t:animalAegithalos_caudatus:site
nsity of ano.t:animalAegithalos_caudatus:si
0.00
-0.10
20000
60000
100000
Iterations
0
5
10
20
-0.10
-0.05
0.00
0.05
N = 10000 Bandwidth = 0.003233

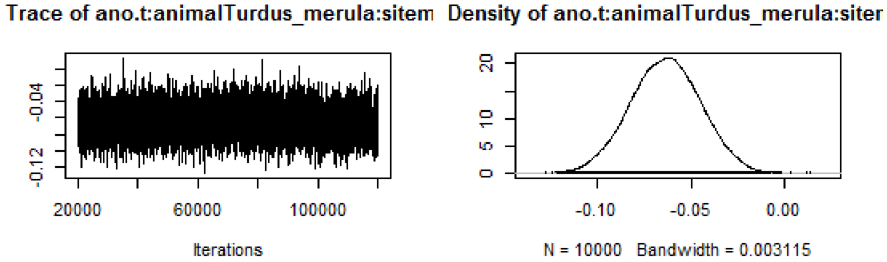
Trace of ano.t:animalTurdus_merula:sitem
Density of ano.t:animalTurdus_merula:siter
-0.04
-0.12
20000
60000
100000
Iterations
0
5
10
20
-0.10
-0.05
0.00
N = 10000 Bandwidth = 0.003115

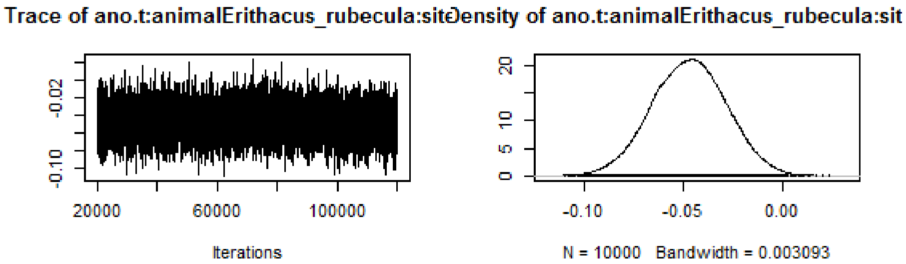
Trace of ano.t:animalErithacus_rubecula:site
Density of ano.t:animalErithacus_rubecula:sit
-0.02
-0.10
20000
60000
100000
Iterations
0
5
10
20
-0.10
-0.05
0.00
N = 10000 Bandwidth = 0.003093

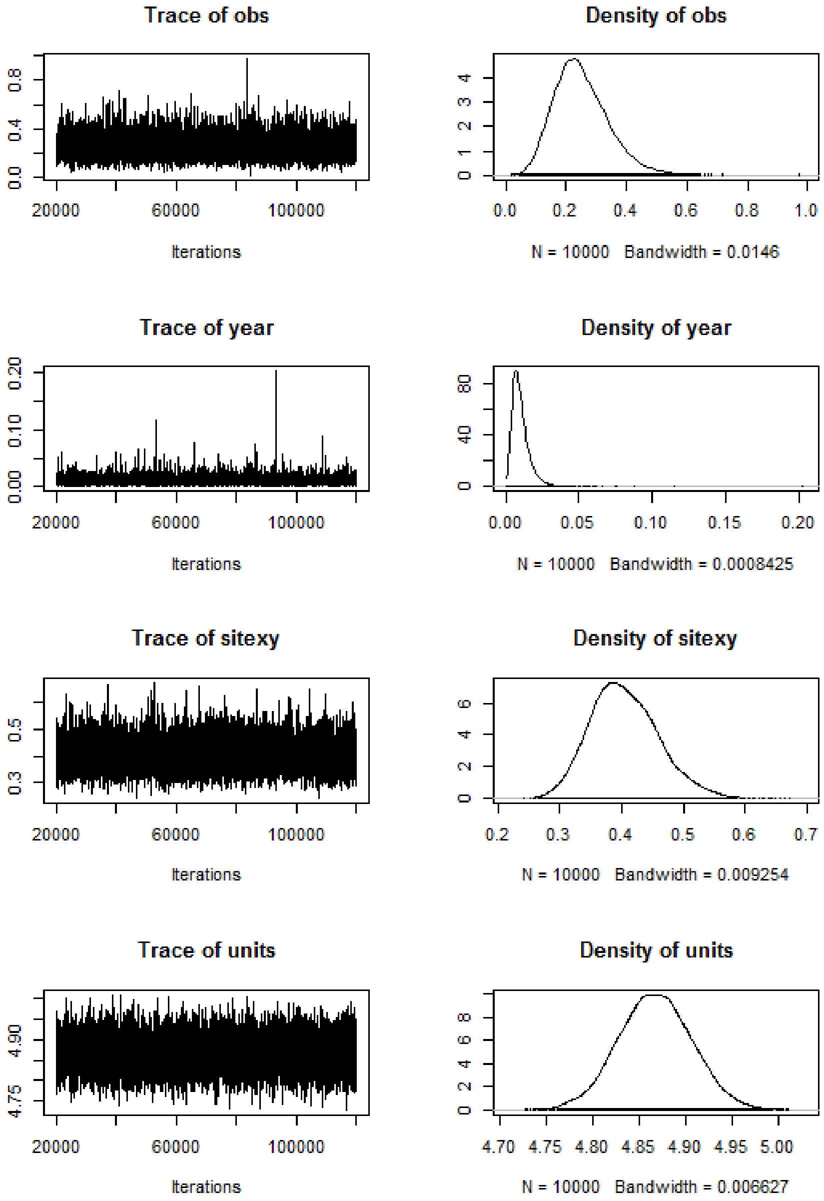
Trace of obs
0.0
0.4
0.8
20000
60000
100000
Iterations
Density of obs
0
1
2
3
4
0.0
0.2
0.4
0.6
0.8
1.0
N = 10000 Bandwidth = 0.0146
Trace of year
0.00
0.10
0.20
20000
60000
100000
Iterations
Density of year
0
40
80
0.00
0.05
0.10
0.15
0.20
N = 10000 Bandwidth = 0.0008425
Trace of sitexy
0.3
0.5
20000
60000
100000
Iterations
Density of sitexy
0
2
4
6
0.2
0.3
0.4
0.5
0.6
0.7
N = 10000 Bandwidth = 0.009254
Trace of units
4.75
4.90
20000
60000
100000
Iterations
Density of units
0
2
4
6
8
4.70
4.75
4.80
4.85
4.90
4.95
5.00
N = 10000 Bandwidth = 0.006627

Appendix S1 List of the 132 observers for which data were used in this study.

Adrien Simon, Allain Antoine, Allard Charlotte, Allard Renaud, Amandine Cardon, Archaux Frederic, Arlaud Cindie, Ballagny Cedric, Baquart Savina, Barth Franz, Batard Romain, Baudoin Christophe, Bauwin Jeremy, Bazir Aissa, Beligne Lea, Bellion Marc, Beltramo Massimiliano, Bergerault Claire, Berjamin Florian, Bertheau Vincent, Bioret Laurent, Blaize Christine, Justine Mougnot, Blondel Lucie, Bosquet Marie, Bouligand Delphine, Bouligand Sandrine, Bouzendorf Emeline, Bouzendorf Francois, Brilland Yan, Broutin Aurelie, Callard Benjamin, Calmon Benjamin, Caron Nicolas Pierre, Chancelier Charley, Chatton Thomas Botte Guillaume, Cheminel Jean Marie, Chevalier Marie, Chil Jean Luc, Cochard Guillaume, Colin Lambert, Corentin Morvan, Corona Sebastien, Couillens Bertrand, Courant Sylvain, David Yves, Debeneste Etienne, Debrabant Charlotte, Dedrie Maud, Defives Pauline, Delamaere Marie, Delanoe Claire, Delecour Vincent, Delliaux Steeven, Denise Cyril, Derolez Bruno, Desailly Pernelle, Dominique Bauvais, Dorfiac Matthieu, Duhayer Jeanne, Dupriez Quentin, Dutilleul Simon, Elise Delagree, Enrique Sans, Farges Romain, Faure Baptiste, Faustine Simon Ilse Gilles Leguillou Yannick Jacob, Fenart Beghin Eric, Fontaine Benoit, Fonteneau Frederic, Fourcade Jean Marc, Francois Gabillard, Francois Hemery, Francois Jeanne, Franz Barth, Gabillard Francois, Gautier Maxime, Gergaud Antoine, Giraud Gest Marine, Gore Olivier, Gouello Thomas, Guet Mathilde, Guillo Jean Claude, Guitton Sandrine, Hanotel Remi, Hemery David, Hemery Francois, Henry Pierre-Yves, Henry Remi, Heroguel Clement, Herrmann Valentine, Herve Gauche, Huchin Francois, Jeanne Francois, Jerome Hanol, Johanna Chopin, Julien Bensliman, Kolon Izabella, Lagarde Marie, Landeau Remi, Latraube Franck, Laurensic Christopher, Laval Benoit, Le Neve Arnaud, Lechat David, Ledunois Romain, Lemaitre Pier Luigi, Lorrilliere Christian, Lovigny Bernard, Magne Jean Francois, Maheu Berengere, Maingueneau Jeremy, Martin Leo, Masquelier Julien, Massuir Philippe, Max Richer, Maxime Jouve Herve Gauche, Maxime Spagnol, Melin Marie, Moal Gael, Monchatre Robin, Monnier Gildas, Mortreux Stephane, Motteau Valentin, Mougeot Nicolas, Mougnot Justine, Moussus Jean Pierre, Nade Philippe, Paoli Jerome, Paquin Frederique, Perignon Laurent, Perroi Pierre Yves, Pichard Adeline, Pierre Thellier, Pincon Sylvain, Poncet Sophie, Provost Romain, Regnier Ma, Regnier Marie Claire, Remond Elodie, Renaud Regine, Robbe Eric, Rolland Simon, Romain Lengagne, Rumianowski Odin, Senecal Didier, Sibler Francois, Soubielle Francois, Sourdrille Kevin, Staphan Jacob, Sylvain Fromet, Sylvain Vincent, Toulotte Fabien, Urbina Patrice, Vaidie Frederic, Viallet Melchior, Vigour David, Yves David, Zucchet Olivier.